International Journal of Extreme Manufacturing

TOPICAL REVIEW • OPEN ACCESS

Bioinspired micro/nanostructured surfaces prepared by femtosecond laser direct writing for multi-functional applications

OPEN ACCESS
IOP Publishing | IMMT
International Journal of Extreme Manufacturing
Int. J. Extrem. Manuf. **2** (2020) 032002 (21pp)
https://doi.org/10.1088/2631-7990/ab95f6

Topical Review

Bioinspired micro/nanostructured surfaces prepared by femtosecond laser direct writing for multi-functional applications

Yiyuan Zhang[1], Yunlong Jiao[1,2,4], Chuanzong Li[3], Chao Chen[1], Jiawen Li[1], Yanlei Hu[1], Dong Wu[1,4] and Jiaru Chu[1]

[1] Key Laboratory of Precision Scientific Instrumentation of Anhui Higher Education Institutes, CAS Key Laboratory of Mechanical Behavior and Design of Materials, Department of Precision Machinery and Precision Instrumentation, University of Science and Technology of China, Hefei 230026, People's Republic of China
[2] Institute of Tribology, Hefei University of Technology, Hefei 230009, People's Republic of China
[3] School of Instrument Science and Opto-Eelectronics Engineering, Hefei University of Technology, Hefei 230009, People's Republic of China

E-mail: jyljjw@ustc.edu.cn and dongwu@ustc.edu.cn

Received 4 March 2020, revised 21 April 2020
Accepted for publication 23 May 2020
Published 9 July 2020

Abstract

Femtosecond laser direct writing (FLDW) has been widely employed in controllable manufacturing of biomimetic micro/nanostructures due to its specific advantages including high precision, simplicity, and compatibility for diverse materials in comparison with other methods (e.g. ion etching, sol-gel process, chemical vapor deposition, template method, and self-assembly). These biomimetic micro/nanostructured surfaces are of significant interest for academic and industrial research due to their wide range of potential applications, including self-cleaning surfaces, oil-water separation, and fog collection. This review presents the inherent relationship between natural organisms, fabrication methods, micro/nanostructures and their potential applications. Thereafter, we throw a list of current fabrication strategies so as to highlight the advantages of FLDW in manufacturing bioinspired microstructured surfaces. Subsequently, we summarize a variety of typical bioinspired designs (e.g. lotus leaf, pitcher plant, rice leaf, butterfly wings, etc) for diverse multifunctional micro/nanostructures through extreme femtosecond laser processing technology. Based on the principle of interfacial chemistry and geometrical optics, we discuss the potential applications of these functional micro/nanostructures and assess the underlying challenges and opportunities in the extreme fabrication of bioinspired micro/nanostructures by FLDW. This review concludes with a follow up and an outlook of femtosecond laser processing in biomimetic domains.

[4] Authors to whom any correspondence should be addressed.

2631-7990/20/032002+21$33.00

Keywords: femtosecond laser direct writing, multiscale micro/nanostructures, extreme fabrication, bioinspired applications

1. Introduction

Nature often guides the practical applications of modern industrial extreme manufacturing [1–5]. As a results, bioinspired design from natural organisms, that exhibit extreme functional characteristics arising from their unique surface micro/nanostructures, have been implemented in radars [6], submarines [7], and airplanes [8–12], to obtain useful functionalities such as anti-wear [13], anti-corrosion [14], and self-cleaning [15–21]. One of the most attractive phenomena is the self-cleaning ability of lotus leaf, which as the poem by Dunyi Zhou says 'She grows in mud, yet never contaminates with it. She floats on waving water, yet never dances with it'. The second paradigm is Namib desert beetles can survive in extremely dry and foggy deserts, which has implications for reducing fog in airports, collecting water for irrigation and collecting potable water in foggy, arid environments. These extreme biological characteristics possess unique surface topography and proper intrinsic wettability. The fluff and tiny-nanoscaled waxy particles endow the surface of the lotus leaf with superhydrophobic characteristics and self-cleaning capability. The combination of the superhydrophilic texture and superhydrophobic grooves on the surface of Namib desert beetles render their capability of sucking water vapor from moist air. As abundant water droplets accumulate in the superhydrophilic regions, they roll along the bow back and fall into the beetle's mouth.

In order to obtain these functional micro/nanostructured surfaces, researchers have developed diverse micro/nanoprocessing methods, including reactive ion etching, sol-gel processing, chemical vapor deposition, electrochemical processing, template methods, self-assembly etc [22–30]. Unfortunately, these methods suffer from limitations. For instance, the processing steps are too complicated to control precisely; the processing platforms are limited to the specific materials; the processing environment is harsh; the fabrication process is always accompanied by secondary pollution and so is not environment-friendly. There is still an urgent need for new strategies of preparing biomimetic multifunctional surface micro/nanostructures efficiently, accurately, and easily. As a novel method of preparing micro/nanostructures, femtosecond laser direct writing (FLDW) technology has attracted great attention due to its ultrahigh processing accuracy, wide application for various materials, simplicity, and rapidity. Many reviews have reported the tremendous achievements of the FLDW technology towards advancing the field of micro/nanofabrication [31–33]. However, essential characteristics, such as the classification, formation mechanism, and design paradigm, of specific extreme micro/nanostructures have not been systematically summarized. A deep understanding of these essential characteristics is vitally important to the fabrication of biomimetic surface morphology through FLDW.

In this review, we present the correlation among natural organisms, fabrication methods, micro/nanostructures and potential applications. Then we compare the features of existing fabrication strategies and highlight the advantages of FLDW in preparing bioinspired microstructures. Subsequently, we present the bioinspired designs (e.g. lotus leaf, pitcher plant, rice leaf, butterfly wings, etc) and extreme femtosecond laser processing of diverse multifunctional micro/nanostructures (e.g. microhole, micropillar, hierarchical structure, nanoripple, self-growing structure). Based on the principle of interfacial chemistry and geometrical optics, we summarize the applications of various micro/nanostructures prepared by FLDW in the fields of structural color, self-cleaning, oil-water separation, fog harvesting, underwater bubble collection, droplet directional transport, and droplet/optical switch. Finally, we conclude with a summary of the challenges and opportunities associated with fabricating bioinspired micro/nanostructures by FLDW and an analysis of the future of femtosecond laser processing in biomimetic field.

2. Correlations among nature organisms, fabrication methods, micro/nanostructures and potential applications

Natural organisms have developed micro/nanostructures with tremendous attractive capabilities which induces abundant intriguing inspirations for human to utilize micro/nanofabrication methods to assimilate and/or emulate to develop diverse potential applications (figure 1). For instance, self-cleaning surfaces were inspired by the natural lotus leaf, which emerges from the mud unstained [34]. The compound-eye camera was inspired by the dragonfly's compound eyes, which enable wide angle reconnaissance [35]. Structural coloration was inspired by butterfly wings, which produce brilliant iridescent colors when illuminated by the moonlight [36]. Dry tape was inspired by the gecko foot, which can grip even the slipperiest surfaces, giving rise to the lizards exceptional climbing abilities [37]. These biological functions have provided great impetus for scientists to develop similarly functional materials.

The hierarchical structure at the micro/nanoscale is recognized as the key element in determining the reproduction of these unique functions [38–43]. For example, covering multiscale micro/nanostructures in a thin layer of hydrophobic wax prevents pollutants from adhering to surfaces similar to the self-cleaning lotus leaf. Dust particles could be easily removed when liquid droplets roll over a lotus leaf, which is

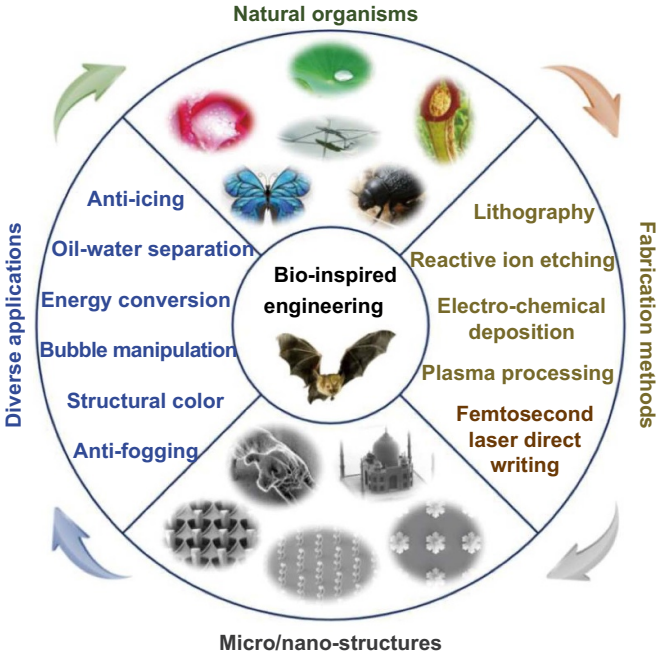

Figure 1. Correlations among nature organisms (bats [57], lotus leaf [58], water strider [59], rose petal [60], pitcher plant [61], butterfly wings [62] and desert beetle [63]), fabrication methods (lithography [64], reactive ion etching [65], electrochemical deposition [66], plasma processing [67] and femtosecond laser direct writing [68]), micro/nanostructures [69–73] and potential applications (anti-icing [74], oil-water separation [75], energy conversion [76], bubble manipulation [77], structural color [78] and anti-fogging [79]).

defined as the self-cleaning effect. In addition, the superhydrophobic leaf surface with multiscale micro/nanostructures exhibits a high adhesion force to the air bubbles in liquid (superaerophilicity), which could be used for the collection of desirable energy-rich gases from the deep sea [44].

Moreover, various functionalities, including oil-water separation and self-driving fog collection, are closely related to the superwetting performance of the hierarchically structured surface [45]. One of the most important typical surfaces is the single-layered Janus membrane with gradient conical microhole arrays, which shows different degrees of wettability on either side of the membrane. Droplets spontaneously pass through the conical microholes depending on the wetting driving force and the Laplace pressure difference. The bioinspired Janus membrane holds great potential for applications in self-driving fog collection [46].

However, these unique micro/nanostructures present unique challenges for current micro/nanoprocessing methods, including lithography, reactive ion etching, electro-chemical deposition, plasma processing, etc. These traditional methods consist of multistep technology processes that pose severe environmental risks. FLDW technology is a new processing strategy in the field of micro/nanomanufacturing. The femtosecond laser has been utilized to fabricate microstructures on the surface of various materials (e.g. metal [47], polymer [48], etc.). It provides precise control over the size of microstructures by adjusting certain crucial parameters, such as laser power, scanning speed, and scanning period. Through the advanced micro/nanomanufacturing technology, we can replicate the unique biomimetic micro/nanostructures to harvest a variety of functions similar to those observed in natural organisms, including anti-icing [49], oil-water separation [50], energy conversion [51], bubble manipulation [52], structural color [53, 54], and anti-fogging [55, 56].

3. Interaction between femtosecond laser and solid substrate

As one of the most important means for humans to explore the microworld, micro/nanofabrication technology has extremely vital applications in fabricating microelectronics [83], microoptics [84], microfluidics [85], and other leading-edge fields [86–89]. Currently, widely adaptive technologies consist of planar lithography [90], electron beam etching [91], focused ion beam etching [92], chemical polymerization [93], and self-assembly [94] (figure 2). However, these micro/nanofabrication technologies have limited practical applications. For example, lithography is usually used in plane processing. The efficiency of non-plane processing will be significantly reduced (figure 2(a)). The rate and efficiency of reactive ion etching are relatively low. It is difficult to prepare multi-component films by electro chemical deposition, and the growth rate of crystal nuclei cannot be precisely controlled (figure 2(b)). Plasma treatments suffer from poor precision control, resulting in structures with rough surfaces (figure 2(c)). Electron beam etching and focused ion beam etching are expensive methods of micro/nanostructure fabrication. It should be noted that the intrinsic shortcomings of these traditional techniques limit their potential application in diverse fields.

In recent years, femtosecond laser direct micro/nanowriting technology has been widely adopted in the field of micro/nanomanufacturing (figure 2(d)) [95]. Due to its extremely short pulse width, a femtosecond laser can achieve extremely high peak power at the focal spot, even if the pulse energy is only in the order of microjoule or millijoule. Under strong light field conditions, the electric field intensity of the laser can distort the coulomb potential of most neutral atoms, causing a nonlinear interaction between light and matter, such as multi-photon absorption or tunneling ionization [96]. Compared with other micro/nanowriting technology that utilizes nanosecond pulsed light or continuous laser [97], FLDW offers several unique advantages: (1) high processing accuracy due to its relatively low thermal impact in the processing area; (2) high peak intensity, which makes FLDW processing suitable for almost any; (3) high processing resolution, especially for two photon polymerization because of the femtosecond nonlinear absorption effect; (4) the femtosecond laser has a long wavelength and excellent penetrability, making it suitable for true 3D fabrication. The mechanism of femtosecond laser induced controllable multiscale micro/nanostructures is related to three effects: laser ablation effect [98], laser-induced effect [99], and debris self-deposition [100].

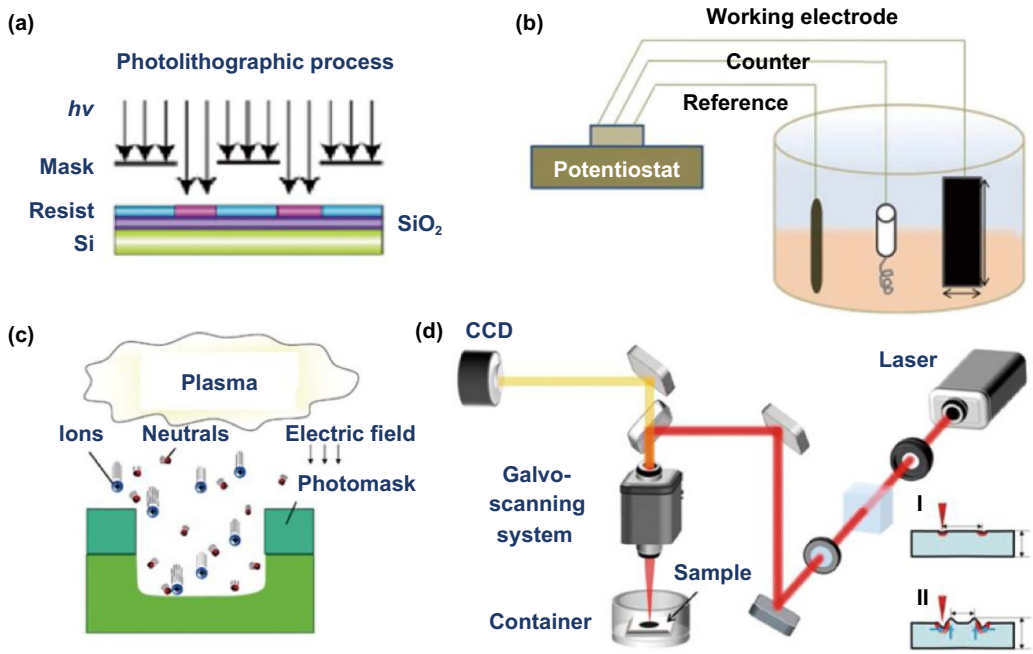

Figure 2. Diverse micro/nanofabrication methods. (a) Lithography and etching [80]. (b) Electrochemical deposition [81]. (c) Plasma processing [82]. (d) Femtosecond laser processing technology [114–116]. (a) [111] (2010) With permission of Springer. (b) Reprinted from [112], Copyright (2014), with permission from Elsevier. (c) Reproduced from [113]. © IOP Publishing Ltd. All rights reserved. (d) Reprinted with permission from [114]. Copyright (2015) American Chemical Society.

(1) Under the laser irradiation, the target material absorbs the laser energy and transforms into a liquid or gas. The molten liquid is expelled from the zone of action by recoil. The steam escapes directly from the focal point. During the process, some nanoparticles form around micropits, which result from the combined effects of laser shock compression and debris deposition [101]. Due to the short pulse width in the process of femtosecond laser induction, the vapor and plasma phases are rapidly generated with negligible conduction, and no liquid phase presents [102]. It is worth noting that the laser ablation effect contributes to the fabrication of various microscale structures (e.g. microhole, micropillar, and microgroove). At the same time, the nanoscale structures (e.g. nanoparticle) are also generated around the microscale structures due to the debris self-deposition effect [103].

(2) Another fabrication mechanism of surface structure is mainly derived from the laser-induced effect. The theories for the generation of periodic fringe structure induced by ultrashort pulse laser include self-organization [104], plasma excitation [105], and second harmonic generation [106]. Electromagnetic field energy of the incident plan wave does not distribute evenly on thin, rough surfaces (note that the surface thickness is much smaller than the wavelength of the incident light). The electromagnetic field energy distribution [107] determines the formation of periodic self-organizing fringe [107]. Periodic ripples are among the important induced fringe structures, and are widely employed in the manufacturing of special wettability surfaces [108] and metal coloring [109].

(3) Under the condition of liquid-assisted (source solution [110], ethanol [111], water [112] and so on) processing, femtosecond laser processing could produce unique structures different from those produced in an open-air environment. It should be noted that the fabrication process of liquid-assisted FLDW is more complex, consisting of five general phases, including laser-induced plasma effect of liquid, enhanced heat conduction, increased shock wave, intensified acoustic pressure, and explosive vaporization. The femtosecond laser may produce a superheated substance [113] around the target sample, which brings the surrounding liquid to a supercritical state [107]. The resulting pressure wave interacts with the liquid layer on the target surface, altering its morphology. The forming mechanism of mico/nanostructures fabricated by liquid-assisted FLDW is mainly related to the ultrahigh temperature of plasma ions excited at the liquid/solid interface, and the capillary wave during the cooling process. Additionally, the ablation process generates smaller bubbles around the target sample. The interaction between the liquid, bubble, and solid surface plays a critical role in the fabrication of specific micro/nanostructures.

In short, FLDW is efficient strategy for the fabrication of multi-functional micro/nanostructures. FLDW involves various interactions between the laser pulse and materials (e.g. laser ablation effect, laser-induced effect, and debris self-deposition), which have broad applications in diverse fields, such as surface modification and fabrication of intelligent micro/nano devices.

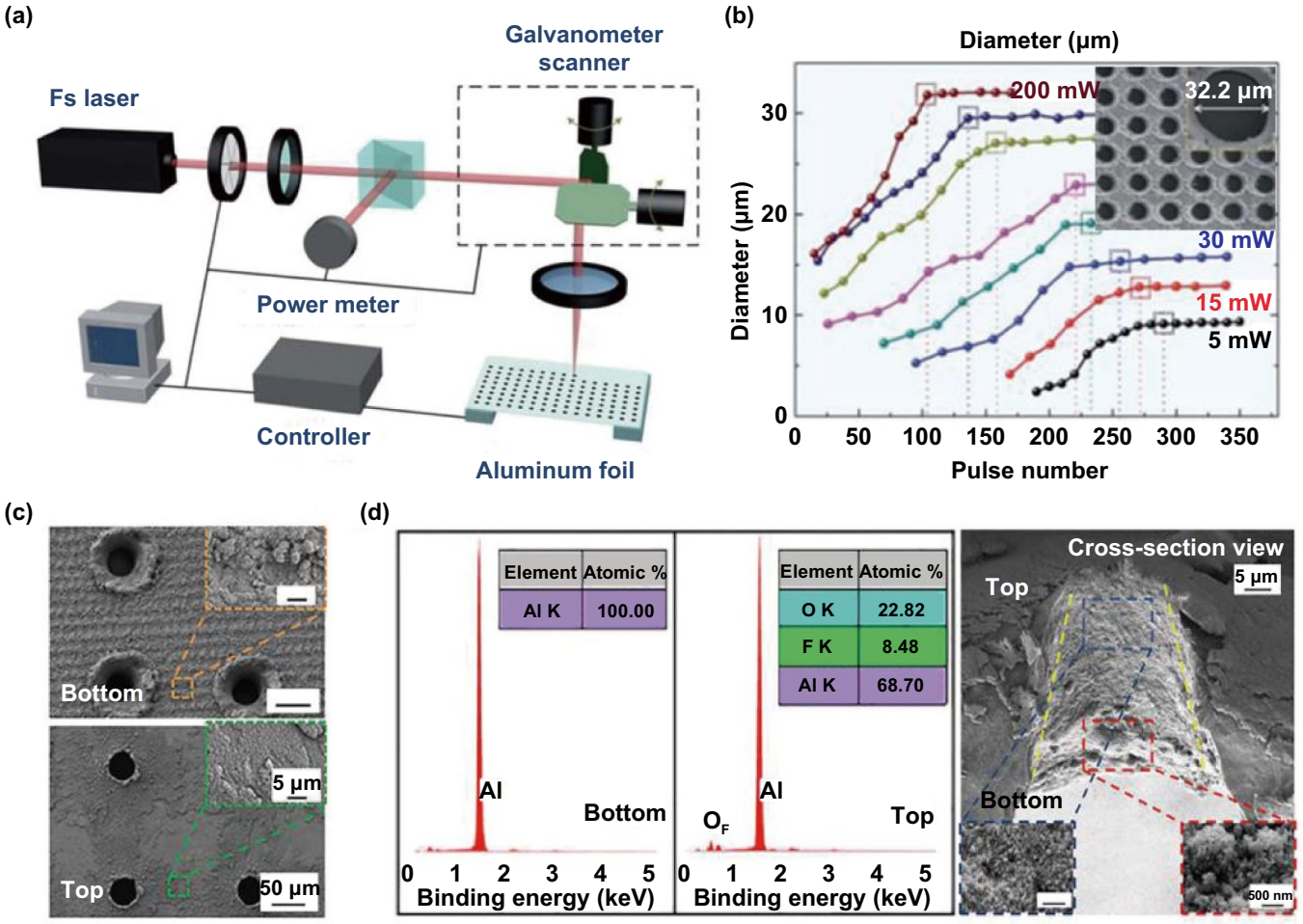

Figure 3. Microhole arrayed structure. (a) Femtosecond laser micro/nanoprocessing system [117]. (b) The relationship between the laser pulse number and the diameter of the microhole under different laser power [117]. (c) The top and bottom SEM images of microhole [118]. (d) The analysis of element composition on the top and bottom of the film after selective laser ablation process. The inside topography of microhole [119]. (a), (b) Reproduced from [117] with permission of The Royal Society of Chemistry. (c), (d) Reprinted from [119], with permission of AIP Publishing.

4. Typical micro/nanostructures by FLDW

4.1. Microhole arrayed structure

The microhole arrayed structure is a typical micro/nanostructure fabricated by femtosecond laser drilling metal or polymer films (figure 3). The inner walls of the microholes drilled by femtosecond laser are smoother and cleaner than those drilled by picosecond or nanosecond laser. For example, Wu *et al* presented a type of regular microhole arrayed aluminum foil ablated by femtosecond laser for efficient oil/water separation (figure 3(a)) [117]. Wu *et al* precisely controlled the diameter of the microholes (2.4 μm–32 μm) by adjusting the laser power and pulse number (figure 3(b)). Chen *et al* designed and fabricated a microhole arrayed Janus PDMS surface based on femtosecond laser drilling to achieve the unidirectional self-transport of underwater bubbles. The microhole diameter could also be precisely controlled by adjusting the laser pulse numbers [115]. Zhang *et al* proposed a simple, functional device for oil/water separation utilizing an aluminum film (oil barrel), covered in an array of tapered microholes induced by femtosecond laser ablation [119]. Recently, Yan *et al* fabricated a Janus aluminum film with tapered microholes using femtosecond laser ablation and selective laser removal of fluorinated areas [118] (figure 3(c)). Yan *et al* reported no fluorine signal on the bottom surface of the film, which indicates that selective femtosecond laser scanning completely removed the fluorination material on the bottom surface (figure 3(d)).

4.2. Micropillar arrayed structure

The micropillar arrayed structure is fabricated by orthogonally decussate line laser scanning on metal or polymeric surfaces. The surface micropillar arrays can be utilized to construct superwetting interfacial materials (figure 4). For instance, taking hints from the underwater superaerophobicity of fish scales, Yong *et al* designed and fabricated multiscale structures on silicon by femtosecond laser [120]. It can be seen from the SEM images that the period and the size of the micromountains was 10 μm and 7–8 μm, respectively. Additionally, there were abundant nanoparticles on each micromountain (figure 4(a)). Chen *et al* manufactured a

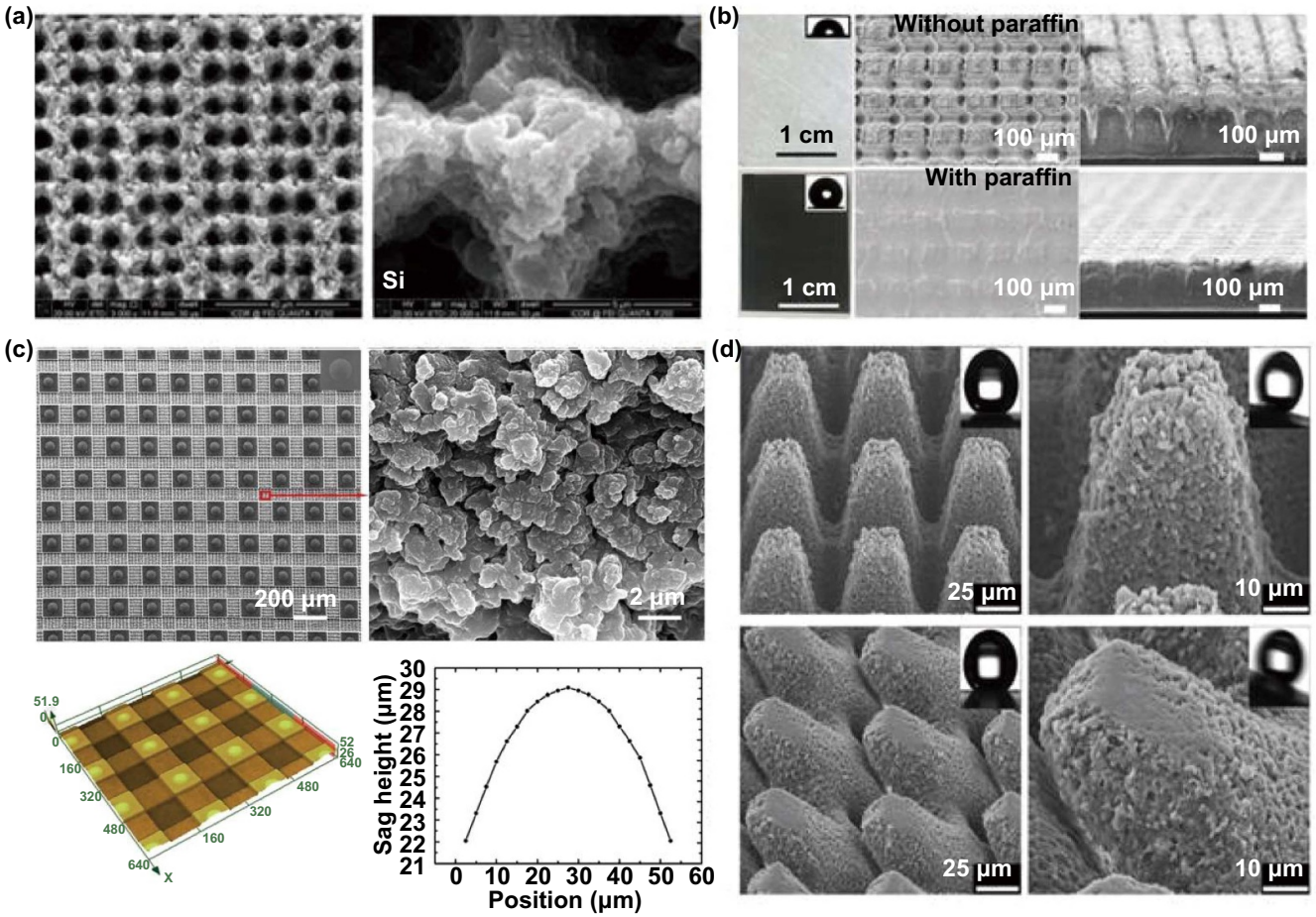

Figure 4. Micropillar arrayed structure. (a) SEM images of silicon surface ablated by femtosecond laser [120]. (b) Digital images of zinc membrane before and after being irradiated by the femtosecond laser [121]. (c) The morphology of the as-prepared microlense arrays [122]. (d) SEM images of the morphology transformation between the upright micropillar arrays and tilted micropillar arrays [123]. (a) Reprinted with permission from [120]. Copyright (2017) American Chemical Society. (b) Reprinted with permission from [121]. Copyright (2019) American Chemical Society. (c) [122] John Wiley & Sons. © 2018 WILEY-VCH Verlag GmbH & Co. KGaA, Weinheim. (d) Reprinted from [123], Copyright (2020), with permission from Elsevier.

hydrophobic micropillar arrayed zinc oxide film (ZOF) using femtosecond laser ablation to realize the *in-situ* reversible tuning of diverse liquids between the sliding and pinning state under ultra-low voltage [121]. It is worth noting that the micropillar arrayed ZOF was covered with paraffin under the effect of capillary force (figure 4(b)). This is the key to achieving dynamic control of droplet movement on the surface, which is confirmed by the sectional and top view of ZOF (figure 4(c)). Moreover, Chen *et al* reported a simple strategy for fabricating superhydrophobic PDMS microlens arrays by wet etching and femtosecond laser direct writing. The fabricated samples exhibited outstanding imaging features and self-cleaning functions (figure 4(c)) [122]. Their research team recently utilized femtosecond laser to prepare hierarchical micropillar arrays (diameter ~ 20 μm, height ~ 45 μm, space ~ 40 μm) on shape-memory polymers, which imparted the surface with superhydrophobicty. The micropillar array could realize the reversible tuning between the tilted and upright state under the heating condition (figure 4(d)).

4.3. Micro/nano hierarchical structure

Micro/nano hierarchical structure is a type of composite structure that contains both microscale and nanoscale structural components, which plays a key role in the preparation of extreme wetting surfaces (e.g. superhydrophobicty, superhydrophilicity). In general, a single microstructure or nanostructure may exhibit hydrophobic characteristics, but its rolling angle is relatively high on account of the high adhesion. Only the surfaces with composite micro/nanostructures (e.g. rice leaf and lotus leaf) can impart a lower adhesion force between droplets and the solid surface, achieving a lower rolling angle ($<10^{\circ}$) and a higher contact angle of droplets ($>150^{\circ}$). Lu *et al* reported a simple and effective method of fabricating hierarchical microgrooved structures on PDMS films by using an energy-tuning laser scanning strategy (figure 5(a)). Firstly, the macrogrooves with anisotropic feature were achieved by laser ablation with large power. The superhydrophobic micro/nanostructures were fabricated under a low laser power.

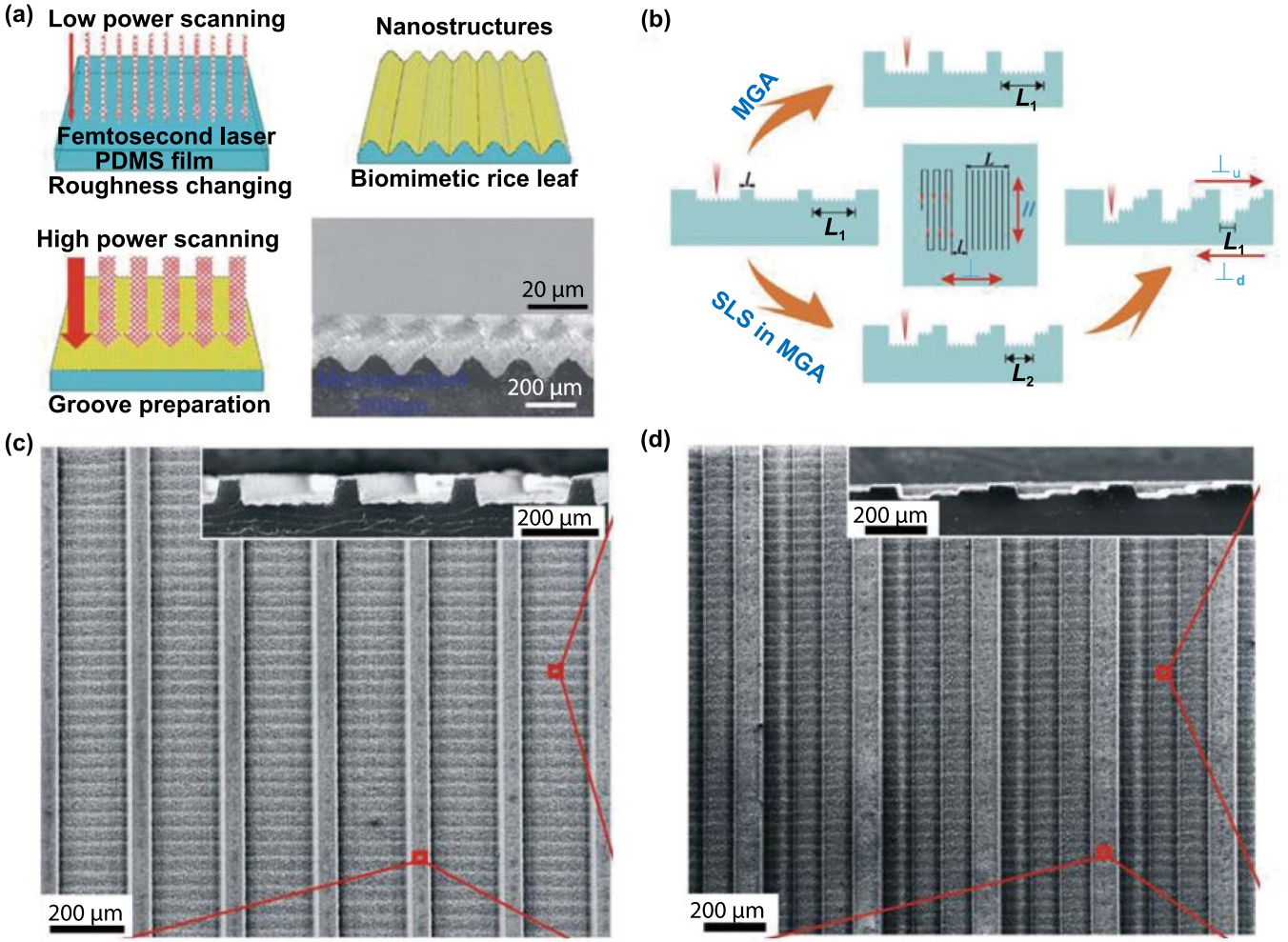

Figure 5. Hierarchical micro/nanostructure. (a) Hierarchical rice leaf surfaces with anisotropic wetting properties and the preparation of the rice leaf-based bioinspired surfaces [124]. (b) Schematic of the femtosecond laser preparation steps for multi-level microstructures. (c) Topological images of microgroove arrays. (d) Topological images of step-like structures in microgroove arrayed surface [125]. (a) Reproduced from [124] with permission of The Royal Society of Chemistry. (b)–(d) [125] John Wiley & Sons. © 2018 WILEY-VCH Verlag GmbH & Co. KGaA, Weinheim.

The as-prepared surface had an obvious anisotropic sliding ability and the difference of sliding angle along the perpendicular and parallel direction was about 6°, which was similar to the real rice leaf [124]. Chen *et al* reported a versatile, bioinspired superhydrophobic surface with tridirectional anisotropic sliding ability (figure 5(b)). They used selective laser processing to constructed the microgroove arrayed PDMS surface, which showed bidirectional anisotropic properties. Additionally, the bidirectional anisotropic ability could be tuned by the height and period of the microgrooves (figures 5(c) and (d) [125].

4.4. *Self-growing structure*

Though bioinspired architectures (e.g. micropillars, microholes, and microcones) have been widely explored, most of these structures are based the material-reducing process during laser ablation. These structures have no shape transformation in a bulk material in response to external stimuli. Recently, Zhang *et al* introduced a 'self-growth' strategy to achieve a localized reconfigurable microstructure transformation on a pre-stretched shape-memory polymeric material through precisely controlling the femtosecond laser ablation (figure 6). These results suggest that it is possible to prepare micropillar structures in one step through the interaction of femtosecond laser with heat-shrinkable polymers (figure 6(a)). Additionally, the as-prepared upright micropillars bend when the laser focus scans another semicircular path (figure 6(b)), which is defined as the asymmetric laser scanning strategy. It is worth noting that the interactions between the laser pulse and the polystyrene materials (e.g. ablation and heating) play an important role in the formation of bent and upright micropillars. On the basis of the mechanical model and analysis (figure 6(c)), the growth mechanism of micropillars consists of four periods as the repeat circles increase. Additionally, various ordered patterns could be achieved by utilizing the bent micropillar as a unit. These intelligent architectures will

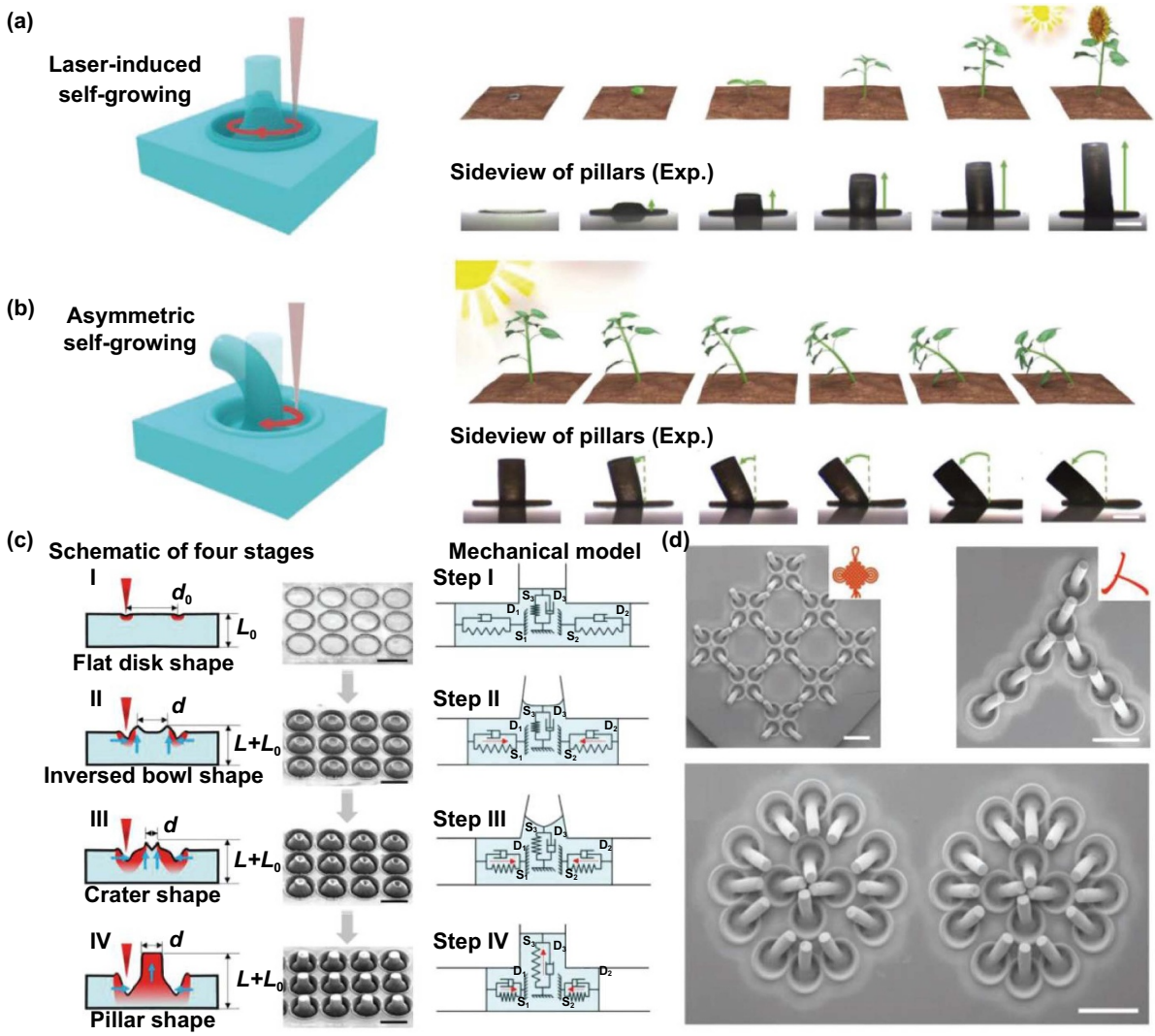

Figure 6. Localized self-growth of reconfigurable architectures [126]. (a) Schematic illustrations of femtosecond laser fabricating SMP film. (b) Schematic illustrations of femtosecond laser processing of the single bent micropillar. Scale bars: 200 μm. (c) Four periods in the process of laser-induced polymer self-growing. Scale bars: 500 μm. (d) Preparation of controllable bent micropillars. (a)–(d) [126] John Wiley & Sons. © 2018 WILEY-VCH Verlag GmbH & Co. KGaA, Weinheim.

find wide applications in industries that rely on information encryption/decryption and particle trapping, such as microstructure printing anti-counterfeiting, and ultrasensitive detection [126].

4.5. Induced nanoripple arrayed structure

The nanoripple arrayed structure is a type of special nanostructure composed of nanometer-wide stripes arranged in a periodic, continuous manner. Nanoripple arrayed structures frequently appear in nature. For example, butterfly wings often contain striped structures arranged periodically. The direct interaction between these structures and incident light endows the butterfly its brilliant colors. It is worth noting that FLDW can induce periodic fringes on the surface of various materials (e. g. metal, semiconductors, and insulators). Studies have revealed that the direction of the periodic stripe is perpendicular to that of the laser polarization. The theories for the generation of periodic fringe structures induced by an ultrashort pulse laser include self-organization, plasma excitation, second harmonic generation, etc. In 2009, Sakabe *et al* divided femtosecond laser induced stripe structure formation into three steps [128]: (1) the femtosecond laser induces plasma waves on the metal surface; (2) the first few pulses of the femtosecond laser forms periodic streaks on the surface and the subsequent process involves a single pulse; (3) the electric field is enhanced at the fringe structure, formed by the subsequent pulse, and then melts the metal surface deepening the periodic structure. As mentioned above, the induced nanoripple arrayed structures are used in the fabrication of special wettability materials and structural color. For instance, Li *et al* used a femtosecond laser micro/nanoprocessing system to achieve structural color applications on stainless steel (figure 7(a)) [127]. The modified surface structure morphology on the stainless steel was detected by a scanning electron microscope (figure 7(b)), which revealed that the ripples,

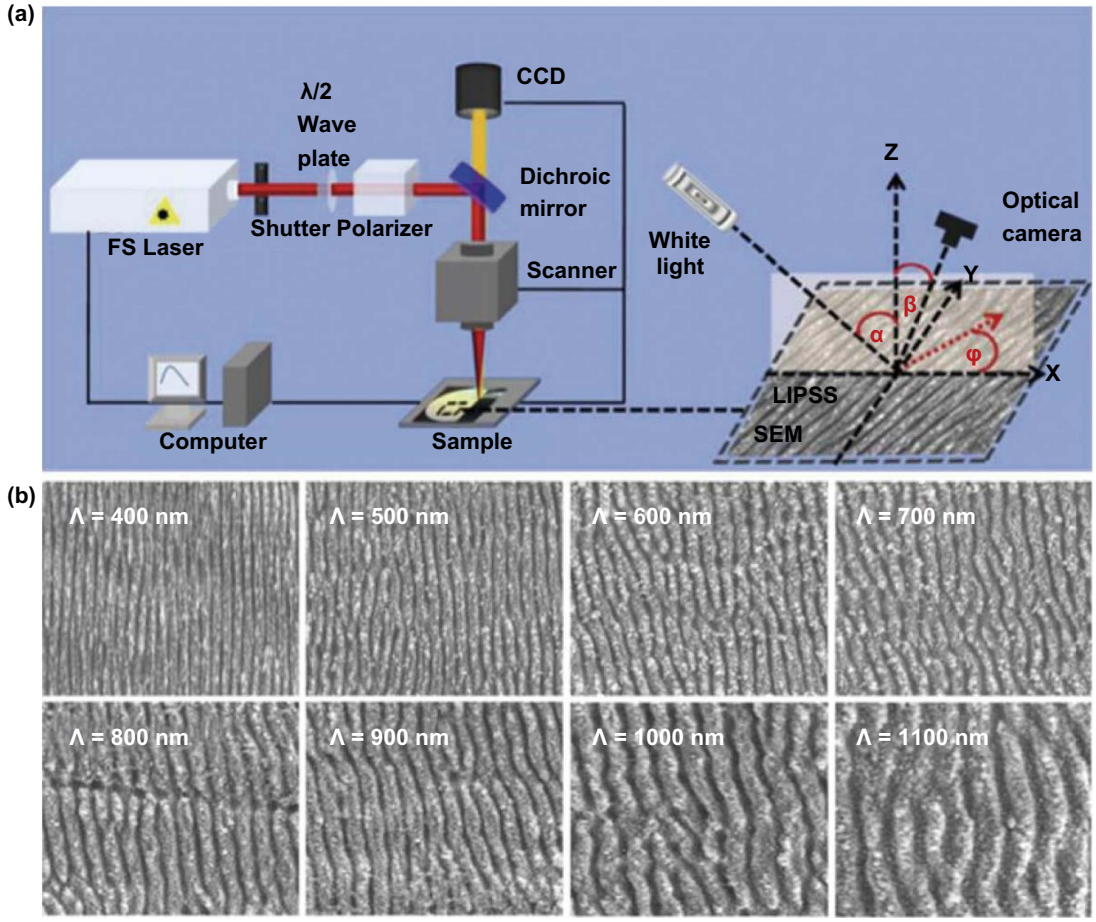

Figure 7. Induced nanoripple arrayed structure. (a) Experimental apparatus for stainless steels fabrication and the schematic of color detecting system [127]. (b) Partial SEM pictures for the laser-induced periodic microstructures by various laser wavelength. (a), (b) [128] (2015) With permission from Springer.

with different periods, could be achieved by various laser wavelengths under suitable laser power and processing speed ranges.

4.6. Other micro/nanostructures induced by liquid-assisted FLDW

Recently, many research groups have focused on liquid-assisted FLDW, which can fabricate distinct micro/nanostructures compared to those created through FLDW in air [129–139]. Li *et al* conducted research on the preparation of various controllable micro/nanostructures by liquid-assisted femtosecond laser ablation [114, 129, 130] (figure 8). They employed different liquids (e.g. ethanol, sucrose, and water) to obtain microcones and micromolar silicon arrays (figures 8(a) and (b)) with tunable wettability. They studied the relationship between the structural parameters (figures 8(c) and (d)), surface roughness (figure 8(e)), and pulse energy to precisely control the microstructure. The formation mechanism of these mico/nanostructures by liquid-assisted FLDW related to the ultrahigh temperature of plasma ions excited at the liquid/solid interface and the capillary wave during the cooling process. It should be noticed that there would generate more and smaller bubbles in water-assisted ablation than that in sucrose solution-assisted ablation. This is because of differences in the viscosity, density, and boiling points of these two liquids, which have enormous effects on the microstructure morphology of silicon.

5. Multi-functional applications of micro/nanostructures

As the fast development of bionics and femtosecond laser extreme processing technology, a variety of powerful interface materials and devices that combine with these extreme micro/nanostructures have been designed and manufactured. These interfacial materials and devices can be adapted to meet diverse functional applications, including oil-water separation, fog harvesting, anti-icing, structural color, droplet and bubble manipulation, and anti-reflection.

5.1. Oil-water separation

Oil-water separation is one of the most crucial technological processes in the oil industry. Due to frequent oil spill accidents, the problems of resource waste and environmental pollution are becoming more and more serious (figure 9). Oil spill

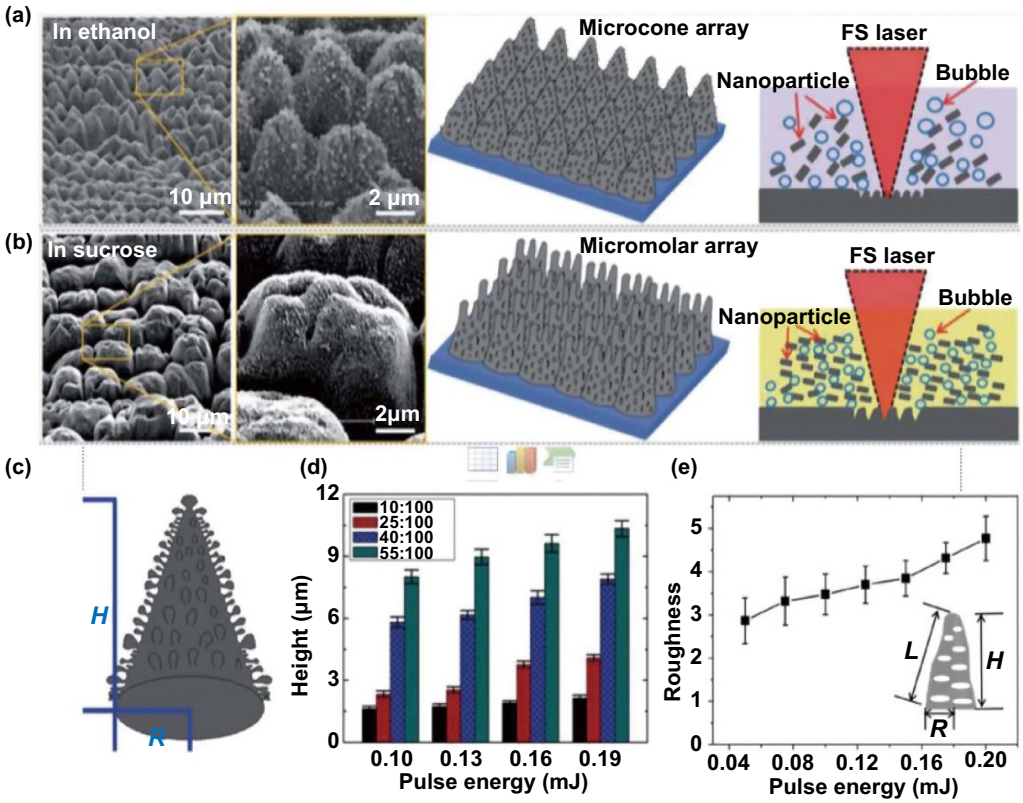

Figure 8. Various microstructures induced by FLDW in liquid. (a) Microcone arrays with ethanol-assisted femtosecond laser ablation [129]. (b) Micromolar arrays with sucrose solution-assisted femtosecond laser ablation [129]. (c) Schematic of the magnified microcone [130]. (d) The statistical height of the microcones, which are obtained through utilizing the average values. At every weight percentage of the sucrose solution, the height increases with the increasing laser power, but the rates of growth are lower [130]. (e) The roughness factors calculated from the data [114]. (a), (b) Reproduced from [129] with permission of The Royal Society of Chemistry. (c) Reproduced from [130] with permission of The Royal Society of Chemistry. (d) Reprinted from [131]. Copyright (2008) American Chemical Society.

accidents severely contaminate and endanger marine ecosystems. In recent years, oil spills have resulted in the deaths of a large number of natural organisms [140]. Researchers have proposed several solutions to solve this issue, including air-float separation [141], gravity separation [142], and centrifugal separation [143]. Oil-water separation materials prepared by femtosecond laser extreme manufacturing methods also show promising results. Wu *et al* reported a Janus oil barrel based on the tapered microhole arrayed aluminum film to achieve spontaneous collection of spilled oil with an ultrahigh flux (45 000 Lm^{-2} h^{-1}) for further oil/water separation [119]. Firstly, femtosecond laser drilling was utilized to prepare the double-faced superhydrophilic aluminum membrane and the diameters of the microholes were precisely regulated by adjusting the laser power and pulse numbers. After the fluorination modification and the selective laser removal of the modification area, the Janus barrel was harvested. Hu *et al* also reported a novel aluminum film covered by large-area regular micropores [117], which performed continuous high-speed oil-water separation and oil collection. Yin *et al* proposed a versatile strategy to prepare stainless steel mesh with periodic nanoripples induced by femtosecond laser, which possess superhydrophilic and underwater superoleophobic properties. The interfacial materials showed robust stability after abrasion tests and longevity tests [144].

5.2. Fog harvesting

Fog harvesting based on bioinspired micro/nanostructured surfaces with specific wetting ability has attracted attention as possible solution to the water shortage plaguing modern society (figure 10). One of the most important bioinspired phenomena is the hump-like surface microstructure inspired by the Namib dessert beetle's back, which possess excellent fog collection capabilities. Ren *et al* designed and fabricated a Janus (hydrophobic/hydrophilic) aluminum film covered by gradient conical micropore arrays for efficient fog collection [116]. It is worth noting that the collection on the Janus film is nearly twice as efficient compared with the original superhydrophilic film, which shows a great potential application in constructing a water collection device to alleviate the freshwater crisis. Inspired by the beetle's elytra, Kostal *et al* utilized a simple three-step preparation strategy to increase the collection efficiency of glasses. It was demonstrated that high-contrast wetting surfaces collected the most fog and increased the fog-collection efficiency by ~ 60% compared to the pristine

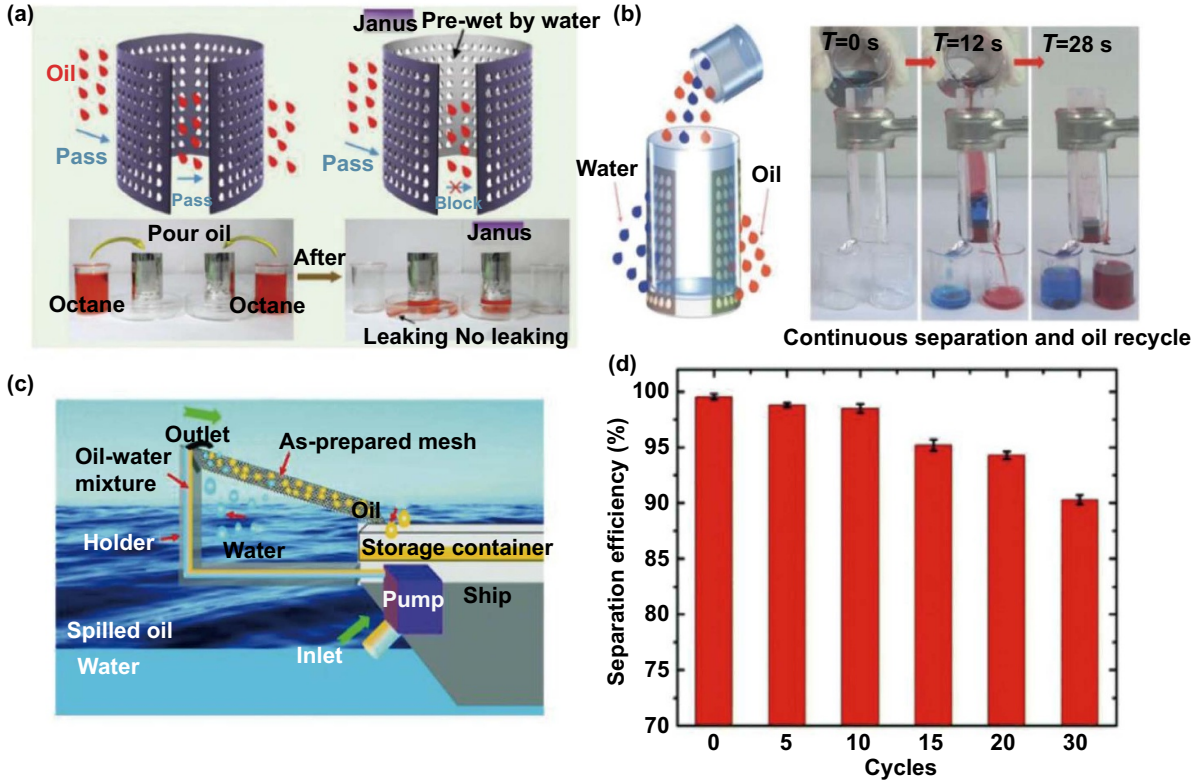

Figure 9. Oil-water separation. (a) Schematic and the optical pictures of the comparison between the Janus barrel and the double-faced superhydrophobic barrel respectively. The Janus barrel is capable of preventing the absorbed oil from leaking again [119]. (b) The autonomous devices for continuously separating oil-water mixtures and the time-lapse pictures of continuous oil-water mixtures separation [117]. (c) Schematic of the as-prepared stainless-steel mesh collection of spilled oil. (d) The separation efficiency of the mesh after 30 recycles of the abrasion test [144]. (a) Reproduced from [118] with permission of The Royal Society of Chemistry. (b) Reproduced from [117] with permission of The Royal Society of Chemistry. (c), (d) Reproduced from [144] with permission of The Royal Society of Chemistry.

Pyres glass [145]. Yin *et al* reported a novel high-efficiency strategy to prepare a Janus microstructured membrane covered with nanoparticles on copper foam by femtosecond laser microfabrication. The fabricated janus membrane was able to collect water in foggy conditions with a maximum collecting efficiency of ~ 3.7 g (cm h)$^{-1}$ [146]. Recently, they also proposed a hybrid hydrophilic-superhydrophobic surface on the copper mesh which contained micro/nanopatterns induced by femtosecond laser ablation [147]. The Janus film based on copper mesh could significantly enhance the fog collection efficiency, which could be controlled by adjusting the inclination angle, mesh number, and surface microstructure. In addition, it was noted that the as-prepared surface exhibited outstanding anti-corrosion ability after immersing it in NaOH, HCl, and NaCl solutions, which may promote its application in water collection.

5.3. Anti-icing

Icing is a common natural phenomenon. Under certain conditions, the attachment and accumulation of snow and ice poses significant economic losses and potential safety hazards. Thick ice on power lines threatens the safe operation of power, railway, and communication networks [148]. Current ice removal methods are summarized as mechanical method [149] and melting strategy [150]. But these methods are utilizing complex structural design and require large amounts of additional energy consumption. Superhydrophobic surfaces have received extensive attention, showing great potential in self-cleaning. The superhydrophobic materials have demonstrated outstanding ice resistance (figure 11). Zhong *et al* studied the underlying mechanism in fabricating surface micro/nanostructures by ultrafast laser [151]. Furthermore, the influences of surface micro/nanostructures on the adhesion, anisotropy, stability and anti-icing performance of superhydrophobic surfaces were systematically studied. There are four kinds of typical hydrophilic nanostructures, whose morphology were mainly decided by the laser scanning parameters, including the scanning interval and pattern. When the hydrophilic metal surfaces were placed in air, they spontaneously turned into highly hydrophobic surfaces due to the adsorption of organic matters onto the metal oxide. It can greatly delay the icing process of surface water droplets under frost-free condition. Under temperatures between −10 ~-6 °C, water droplets on superhydrophobic surfaces maintain their liquid state for 12 h without icing.

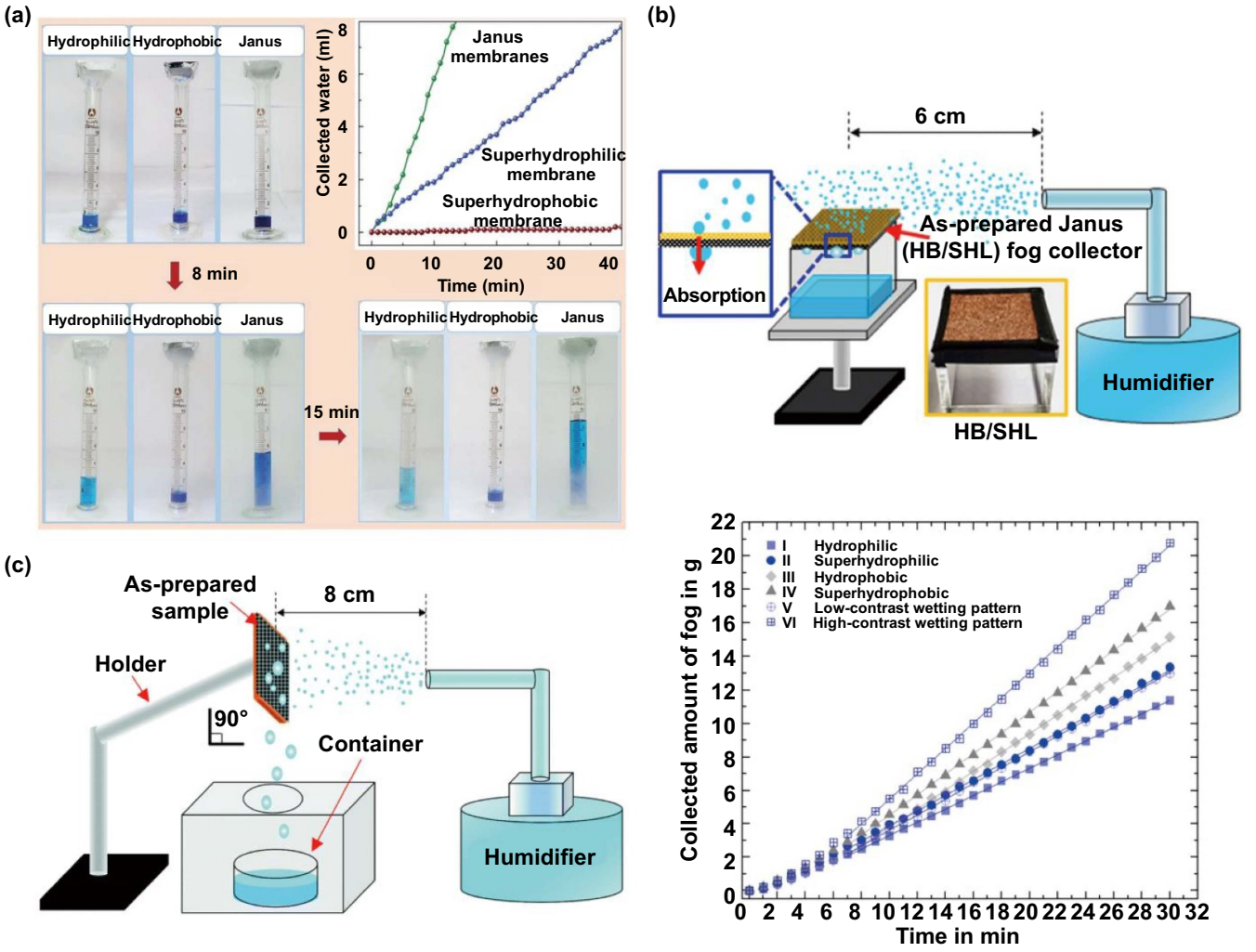

Figure 10. Fog harvesting. (a) The foggy water collection ability of the Janus film compared to two kinds of wetting film. The Janus film shows considerable increase in the collection efficiency [116]. (b) Schematic illustration of the home-made fog-collecting device [146]. (c) Schematic of the purpose-built fog-harvesting device [147]. (d) Collected mass of fog as a function of time [145]. (a) Reproduced from [116] with permission of The Royal Society of Chemistry. (b) Reprinted with permission from [146]. Copyright (2018) American Chemical Society. (c) Reproduced from [147] with permission of The Royal Society of Chemistry. (d) Reprinted with permission from [145]. Copyright (2018) American Chemical Society.

5.4. Structural color

The structural color induced by periodic textures on solid substrates has received great attention in both academic and industrial fields. In most situations, structural color textures are considered a kind of grating structure originating from the diffraction of light (figure 12), which is a simple and vital strategy to change the optical performance of metal surfaces. The surface texturing by femtosecond laser is a versatile and simple way to generate structural colors. For instance, Li and Hu *et al* proposed a strategy to display various colors induced by surface microstructures through simultaneously adjusting the incident light angle and ripple orientation [127]. In addition, different patterns composed of ripples could be precisely designed and controlled by adjusting the incident white light angle and rotating the sample angle. Recently, Wu *et al* reported a microstructured metal surface utilizing a focused laser interference lithography fabrication strategy, which exhibited various structural colors. The water droplet showed an anisotropic wetting ability on the surface. It is worth noting that the fabrication strategy of generating structural color is suitable for multiple materials, such as copper, titanium, iron, etc. Li *et al* proposed controllable parameters (e.g. laser wavelength, spatial period and incline angle) to generate different colors, which could apply to a large range of applications in the art design and laser color marking [152].

5.5. Droplet and bubble manipulation

Droplet and underwater bubble manipulation are vital for both industrial and academic researches due to their practical applications in water treatment, sensors, and microreaction technology. There are several methods (e.g. electric, magnetic, light and thermal actuation) of manipulating the droplet/bubble motion. For instance, electro wetting actuates

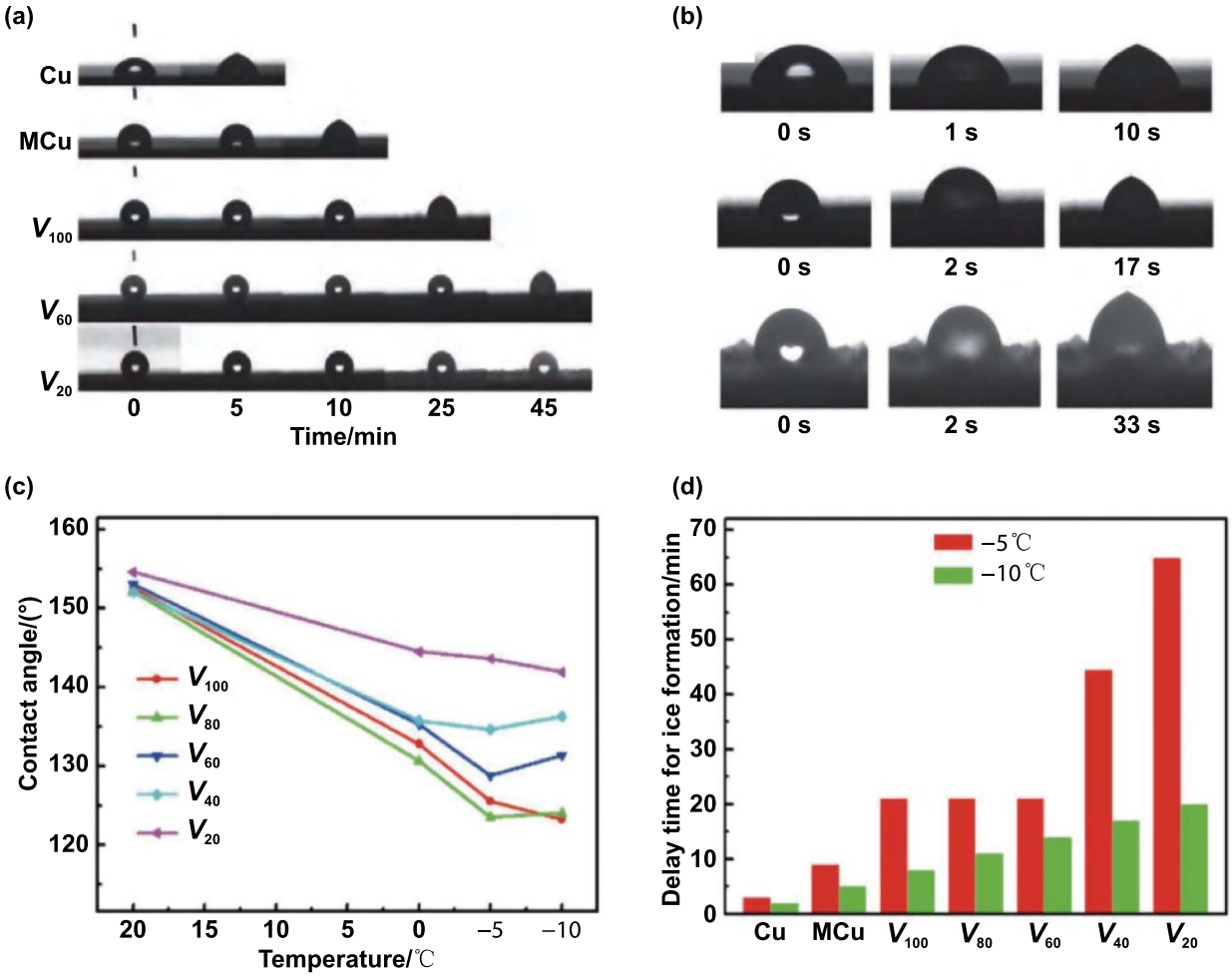

Figure 11. Anti-icing [151]. (a) Ice formation procedure on different Cu sample surfaces. (b) Shape of the droplet on different sampled surfaces before and after freezing. (c) Water contact angle of the superhydrophobic samples fabricated by femtosecond laser versus temperature. (d) Ice information delay time versus samples under different temperatures. (a)–(d) Reproduced with permission from [151].

the droplet motion through the variation of contact angles [153]. The magnetic actuation requires mixing magnetic nanoparticles into the droplets so the droplets respond to external variations in magnetic fields and achieve directional movement [154]. The local temperature of the sample can be significantly altered by thermal stimulus to form a surface tension gradient to actuate the droplet [155]. Moreover, inspired by natural organisms, many functional surfaces with tailored geography and biomimetic microstructures have been artificially realized (figure 13). For instance, Chen *et al* prepared a Fe_3O_4 doped slippery PDMS surface with light response by femtosecond laser crossed ablation [156]. The surface achieved the directional transport of underwater bubbles by loading/discharging a near-infrared light stimulus. The driving mechanism was related to the wettability gradient force due to the high temperature difference. Li *et al* designed an intelligent droplet motion device composed of paraffin wax, micropillar-arrayed zinc oxide film (ZOF) and a flexible silver nanowire heater [121]. The hydrophobic ZOF was fabricated by femtosecond laser ablation. Zhang *et al* designed and prepared an elastic-grooved slippery PDMS surface based on femtosecond laser microfabrication to realize the *in-situ* reversible tuning of droplet sliding movement by mechanical stretch, which was related to the variation of contact angle hysteresis [157]. Jiao prepared a large-area oil infused slippery surface for bubble self-transport and highly efficient gas capture, which was also controlled by the competing forces: resistance (drag force and contact angle hysteresis) and buoyancy [158]. It is worth nothing that differently shaped slippery tracks were prepared to achieve the precise manipulation of underwater bubbles, which may have potential applications in the fields of bubble merging and detachment. Recently, Yong *et al* also reported a porous network of microstructures on different polymer materials [159]. Through the surface modification and oil-infused process, the porous slippery surface showed an outstanding lyophobic ability, which greatly inhibited C6 glioma cells.

5.6. *Anti-reflection*

Functional surfaces and interfaces that reflect minimum electromagnetic waves over a wide spectrum range have vital

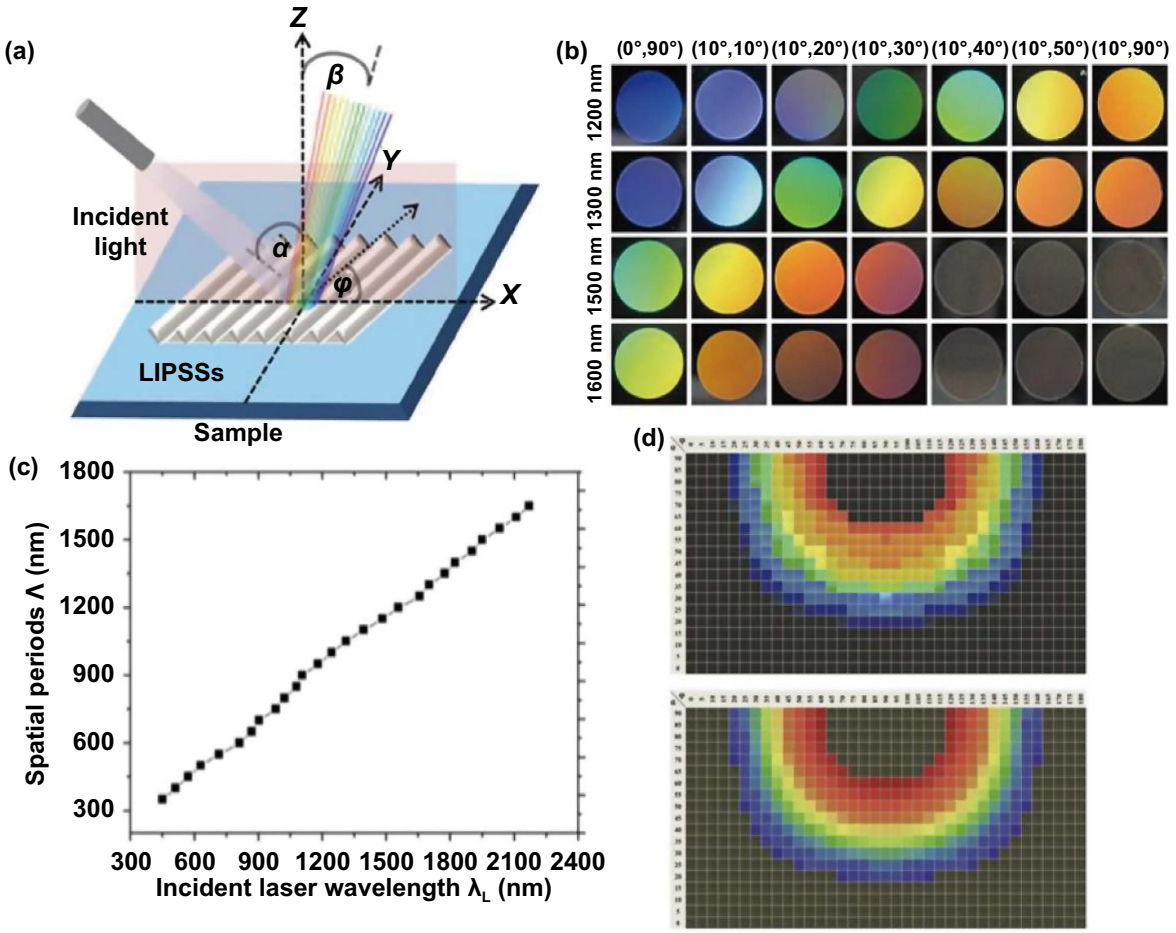

Figure 12. Structural color. (a) Color measurement system. (b) Images of the structural color formed with different structural periods [127]. (c) Structural period of ripples as a function of the laser wavelength [152]. (d) Photographs and simulation consequences of the structural color [128]. (a), (b), (d) Reprinted from [128], Copyright (2015), with permission from Elsevier. (c) Reprinted from [152], Copyright (2014), with permission from Elsevier.

significance for military aircraft equipment. Nevertheless, there are challenges to achieving effective anti-reflection on solid substrates due to the optical impedance mismatch. Most anti-reflection candidate coatings are unable to bridge gaps in the refractive index, which result in the effectiveness of traditional destructive interference coatings and gradient refractive index membranes. Recently, the developed strategies for anti-reflection coatings are limited to non-metal micro/nanostructured materials (figure 14). Zhong *et al* developed a simple strategy for fabricating hybrid anti-reflection micro/nanostructures on different metal surfaces by a femtosecond laser direct writing method [160], which was modified by controlling the laser pulse injection and flexible modifications. Guo *et al* fabricated a versatile large-area grating structure superimposed by finer nanostructures on a silicon surface, which exhibited an anti-reflection effect in the wavelength range from 250 to 2500 nm [161]. These periodic structures induced by femtosecond laser can restrain both the total hemispherical and specular polarized reflectance, which has many advantages, including no environmental contamination and the ability to precisely control the size of the microstructure. Vorobyev *et al* designed the microgroove arrays on silicon substrates covered with nanostructures, which exhibited a significant reflectance reduction [162]. Further investigation suggests that the anti-reflection range can be expanded to the mid-infrared wavelength. For instance, Cheng *et al* designed and fabricated a series of silicon surfaces with textured anti-reflection membranes by femtosecond laser fabrication, which demonstrated a 30% increase of the transmittance response [163].

6. Outlook and conclusion

The fabrication of bioinspired multiscale structures with diverse functions by FLDW has obtained great achievements due to its superior processing characteristics. However, there are still great challenges to face in the FLDW: (1) the interaction mechanism between femtosecond laser and various metallic and non-metallic materials has not been thoroughly studied, and the interaction between some new materials (e.g. shape memory polymer and alloy) and femtosecond laser to produce new structures requires further investigation; (2) femtosecond laser fabrication has some limitations, such as high processing

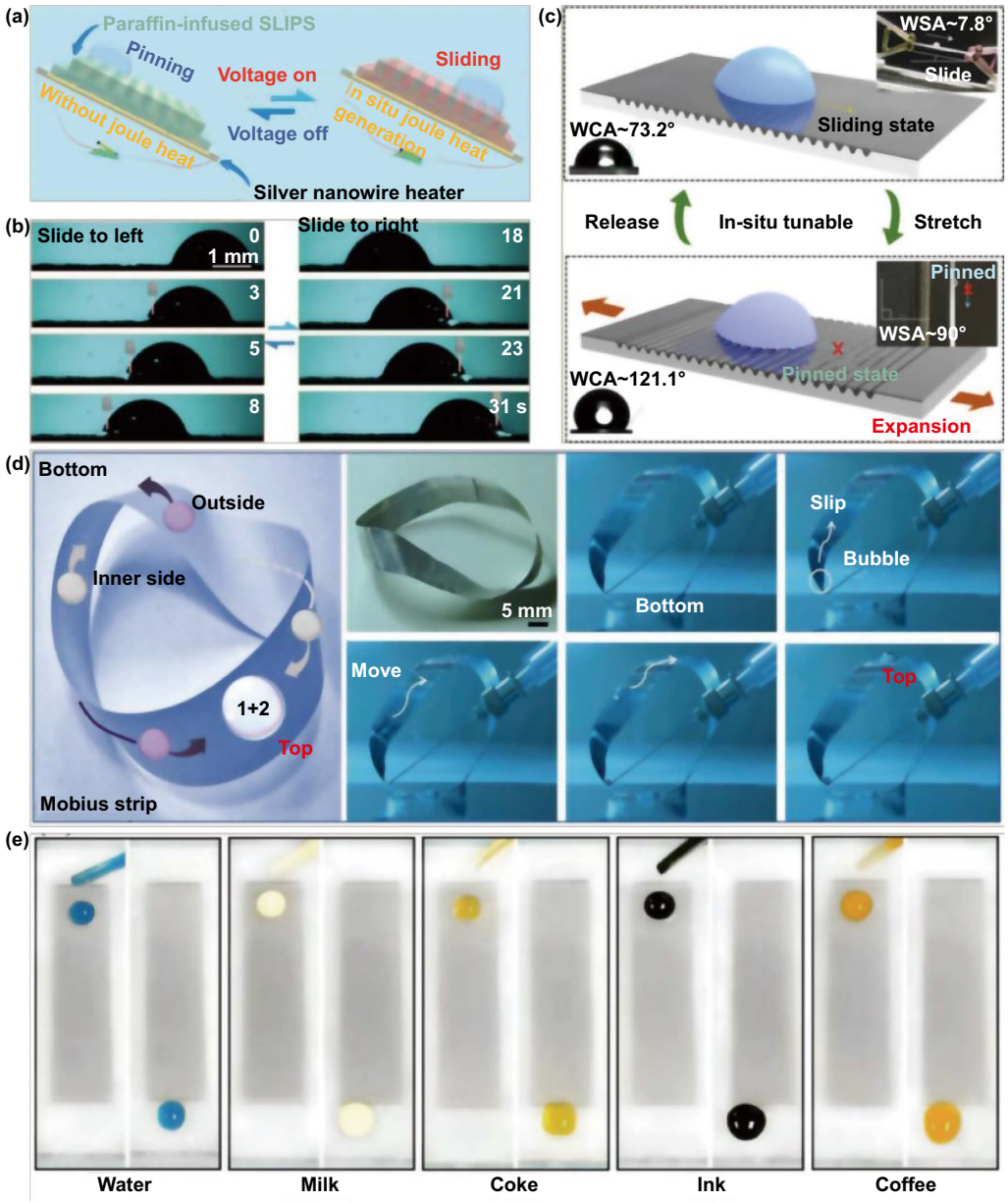

Figure 13. Droplet and bubble manipulation. (a) *In-situ* reversible transformation of droplet motion behavior between pinning and sliding for various liquids actuated by ultralow voltage [121]. (b) The captured time-lapse images for sliding behavior of underwater gas bubble actuated by NIR on SLIPS [156]. (c) Reversible modulation of droplet sliding behavior between pinning and sliding by single-direction stretching the grooved surface [157]. (d) The particular transport process of underwater gas bubble on the Mobius strip-shaped LSS in the 3D space [158]. (e) Pictures of diverse liquids before and after sliding down along the as-fabricated PET sample [159]. (a) Reprinted with permission from [121], Copyright (2019) American Chemical Society. (b) [156] John Wiley & Sons. © 2019 WILEY-VCH Verlag GmbH & Co. KGaA, Weinheim. (c) Reprinted with permission from [157]. Copyright (2019) American Chemical Society. (d) Reproduced from [158] with permission of The Royal Society of Chemistry. (e) [159] John Wiley & Sons. © 2019 WILEY-VCH Verlag GmbH & Co. KGaA, Weinheim.

cost and long processing time, especially in the preparation of large area surfaces for practical applications. Strategies can be provided such as parallel processing of femtosecond laser by programming and high-power laser and high-speed scanning processing; (3) over current research, it is difficult for a single processing method to meet the requirement of achieving the desirable structure and performance, so it is necessary to develop a variety of methods to co-produce biomimetic micro/nanostructures. How to integrate femtosecond laser fabrication technology with other processing methods for achieving the highest efficiency and lowest cost is still an important research question; (4) how to choose the correct structural surface to maximize the application efficiency of the material, such as straight hole arrays or cone hole arrays for oil-water separation is worth studying. Despite the great advances in the technological content, the application of nature-inspired functional surfaces fabricated by FLDW in industrial engineering is still difficult to realize. One of

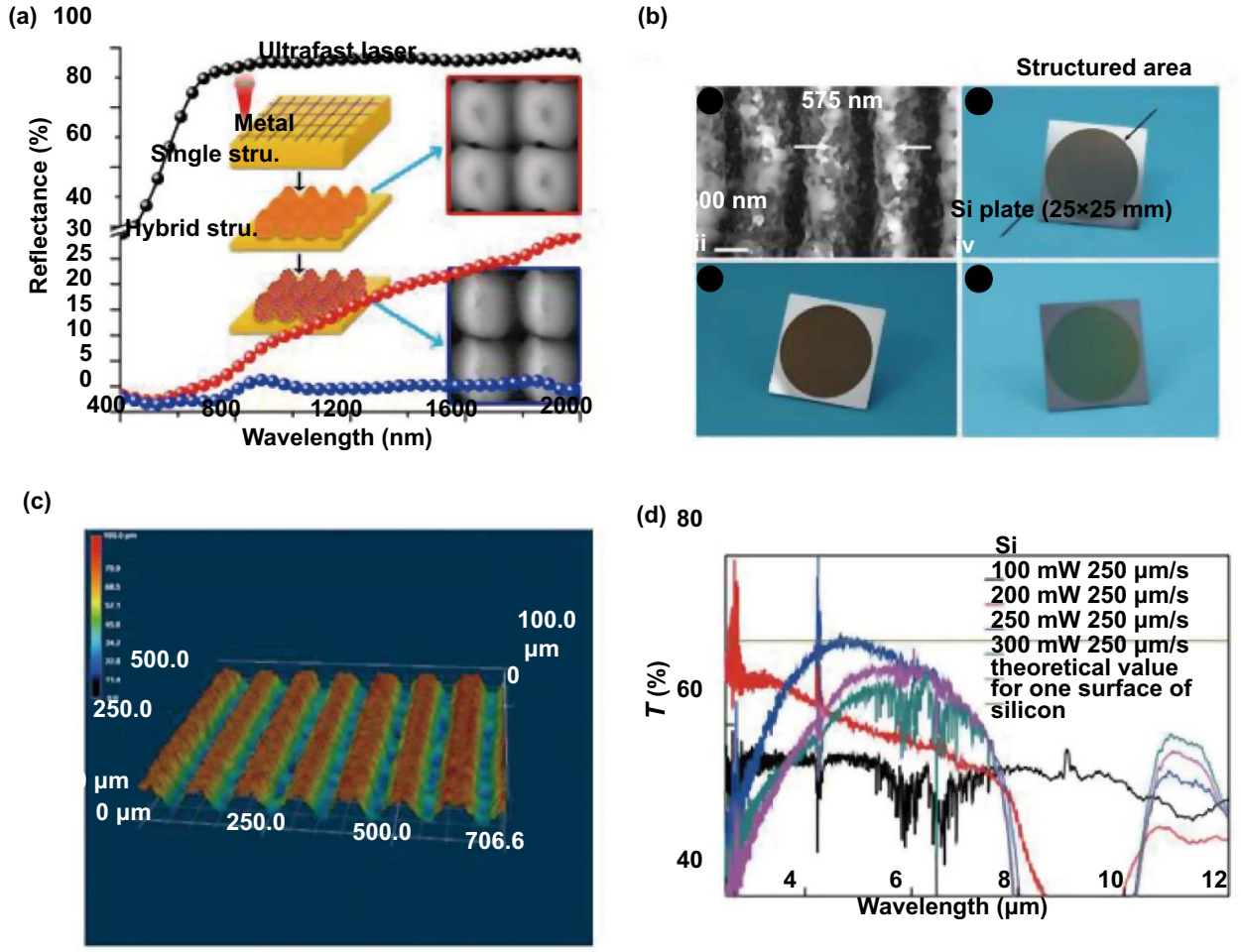

Figure 14. Anti-reflection. (a) Versatile method for dual-scale-controlled micro/nanostructured metallic surface with ultralow reflectance [160]. (b) SEMs of periodic surface structures on silicon induced by femtosecond laser and optical images showing various colors at different detection angles. (c) The three-dimensional optical photograph of the microgrooves on silicon surface [161]. (d) Transmittance of microstructured Si for different conditions [163]. (a) Reprinted with permission from [160]. Copyright (2017) American Chemical Society. (b) Reproduced with permission from [161]. © 2011 Optical Society of America. (c) Reproduced with permissino from [163]. © Chinese Optics Letters.

the key reasons is that the unique ability of these functional materials works well in the laboratory conditions, but could fail in massive industrial production. Therefore, addressing these challenges will advance our fundamental understanding of the mechanisms underlying biological functional surfaces and inform effective methods of producing bioinspired material designs and fabrications for industrial applications.

In this review, we highlighted the utilization of FLDW to achieve the extreme manufacturing of various bioinspired micro/nanostructures, such as microhole, micropillar, hierarchical structure, self-growth structure, and nanoripple. We also summarized crucial applications for laser-ablated micro/nanostructured surfaces in the fields of oil-water separation, anti-icing, fog harvesting, and structural color. It is noteworthy that these nature-inspired functional surfaces have penetrated nearly every aspect of traditional mechanical systems and daily life. However, there is a great step to realize the practical usability of these functional surfaces in massive industrial production by the laser ablated strategy. Through the tireless efforts of broadening the research field of femtosecond laser and deepening the research direction, we believe the femtosecond laser biomimetic structure will be widely-applicable for practical usability in the near future.

Acknowledgment

The present work was supported by the National Natural Science Foundation of China (51 805 508), the Key Project of Equipment Pre-Research Field Fund of China (61 409 230 310), and the Fundamental Research Funds for the Central Universities (WK2090090025).

Author contributions

D W and Y J conceived this review. Y Z and Y J wrote the manuscript and they contributed equally. Y Z, Y J, C L, C C, J L, Y L, D W and J C participated the modification of the manuscript. The authors declare that there is no conflict of interest regarding the publication of this paper.

References

[1] Sanchez C, Arribart H and Guille M M G 2005 Biomimetism and bioinspiration as tools for the design of innovative materials and systems *Nat. Mater.* **4** 277–88

[2] Naleway S E, Porter M M, McKittrick J and Meyers M A 2015 Structural design elements in biological materials: application to bioinspiration *Adv. Mater.* **27** 5455–76

[3] Lauder G V, Madden P G A, Tangorra J L, Anderson E and Baker T V 2011 Bioinspiration from fish for smart material design and function *Smart Mater. Struct.* **20** 094014

[4] Whitesides G M 2015 Bioinspiration: something for everyone *Interfaces Focus* **5** 20150031

[5] Libonati F and Buehler M J 2017 Advanced structural materials by bioinspiration *Adv. Eng. Mater.* **19** 1600787

[6] James R J 1989 A history of radar *IEE Rev.* **35** 343–9

[7] Sun B, Zhu D and Yang S X 2013 A bioinspired filtered backstepping tracking control of 7000-m manned submarine vehicle *IEEE Trans. Ind. Electron.* **61** 3682–93

[8] Weisshaar T A 2013 Morphing aircraft systems: historical perspectives and future challenges *J. Aircr.* **50** 337–53

[9] Ákos Z N M, Leven S and Vicsek T 2010 Thermal soaring flight of birds and unmanned aerial vehicles *Bioinspiration Biomimet.* **5** 045003

[10] Kim J J, Lee Y, Kim H G, Choi K J, Kweon H S, Park S and Jeong K-H 2012 Biologically inspired LED lens from cuticular nanostructures of firefly lantern *Proc. Natl Acad. Sci. USA* **109** 18674–8

[11] Bradley R W, Bombelli P, Rowden S J L and Howe C J 2012 Biological photovoltaics: intra-and extra-cellular electron transport by cyanobacteria *Biochem. Soc. Trans.* **40** 1302–7

[12] Floreano D *et al* 2013 Miniature curved artificial compound eyes *Proc. Natl Acad. Sci. USA* **110** 9267–72

[13] Oh J K, Behmer S T, Marquess R, Yegin C, Scholar E A and Akbulut M 2017 Structural, tribological, and mechanical properties of the hind leg joint of a jumping insect: using katydids to inform bioinspired lubrication systems *Acta Biomater.* **62** 284–92

[14] Payra D, Naito M, Fujii Y, Yamada N L, Hiromoto S and Singh A 2015 Bioinspired adhesive polymer coatings for efficient and versatile corrosion resistance *RSC Adv.* **5** 15977–84

[15] Min W L, Jiang B and Jiang P 2008 Bioinspired self-cleaning antireflection coatings *Adv. Mater.* **20** 3914–8

[16] Bixler G D and Bhushan B 2013 Fluid drag reduction and efficient self-cleaning with rice leaf and butterfly wing bioinspired surfaces *Nanoscale* **5** 7685–710

[17] Nørgaard T and Dacke M 2010 Fog-basking behaviour and water collection efficiency in Namib Desert Darkling Beetles *Front. Zool* **7** 23

[18] Hancock M J, Sekeroglu K and Demirel M C 2012 Bioinspired directional surfaces for adhesion, wetting, and transport *Adv. Funct. Mater.* **22** 2223–34

[19] Wang W, You S J, Gong X B, Qi D P, Chandran B K, Bi L, Cui F and Chen X 2016 Bioinspired nanosucker array for enhancing bioelectricity generation in microbial fuel cells *Adv. Mater.* **28** 270–5

[20] Fu F F, Shang L R, Chen Z Y, Yu Y R and Zhao Y J 2018 Bioinspired living structural color hydrogels *Sci. Rob.* **3** eaar8580

[21] Autumn K, Niewiarowski P H and Puthoff J B 2014 Gecko adhesion as a model system for integrative biology, interdisciplinary science, and bioinspired engineering *Annu. Rev. Ecol. Evol. Syst.* **45** 445–70

[22] Tachi S, Tsujimoto K and Okudaira S 1988 Low-temperature reactive ion etching and microwave plasma etching of silicon *Appl. Phys. Lett.* **52** 616–8

[23] Hench L L and West J K 1990 The sol-gel process *Chem. Rev.* **90** 33–72

[24] Kong J, Cassell A M and Dai H J 1998 Chemical vapor deposition of methane for single-walled carbon nanotubes *Chem. Phys. Lett.* **292** 567–74

[25] Snyder G J, Lim J R, Huang C K and Fleurial J P 2003 Thermoelectric microdevice fabricated by a MEMS-like electrochemical process *Nat. Mater.* **2** 528–31

[26] Martin C R, Van Dyke L S, Cai Z H and Liang W B 1990 Template synthesis of organic microtubules *J. Am. Chem. Soc.* **112** 8976–7

[27] Whitesides G M and Grzybowski B 2002 Self-assembly at all scales *Science* **295** 2418–21

[28] Chou S Y, Krauss P R and Renstrom P J 1996 Nanoimprint lithography *J. Vac. Sci. Technol.* B **14** 4129–33

[29] Xia Y N and Whitesides G M 1998 Soft lithography *Annu. Rev. Mater. Sci.* **28** 153–84

[30] Gattass R R and Mazur E 2008 Femtosecond laser micromachining in transparent materials *Nat. Photon.* **2** 219–25

[31] Yong J L, Chen F, Yang Q, Huo J L and Hou X 2017 Superoleophobic surfaces *Chem. Soc. Rev.* **46** 4168–217

[32] Yong J L, Chen F, Yang Q, Jiang Z D and Hou X 2018 A review of femtosecond-laser-induced underwater superoleophobic surfaces *Adv. Mater. Interfaces* **5** 1701370

[33] Yong J L, Yang Q, Guo C L, Chen F and Hou X 2019 A review of femtosecond laser-structured superhydrophobic or underwater superoleophobic porous surfaces/materials for efficient oil/water separation *RSC Adv.* **9** 12470–95

[34] Marmur A 2004 The lotus effect: superhydrophobicity and metastability *Langmuir* **20** 3517–9

[35] Azuma A and Watanabe T 1988 Flight performance of a dragonfly *J. Exp. Biol.* **137** 221–52

[36] Johnston D and Narayanan R 2008 Active dendrites: colorful wings of the mysterious butterflies *Trends Neurosci.* **31** 309–16

[37] Autumn K, Liang Y A, Hsieh S T, Zesch W, Chan W P, Kenny T W, Fearing R and Full R J 2000 Adhesive force of a single gecko foot-hair *Nature* **405** 681–5

[38] Guo S J and Wang E 2011 Functional micro/nanostructures: simple synthesis and application in sensors, fuel cells, and gene delivery *Acc. Chem. Res.* **44** 491–500

[39] Stratakis E, Ranella A and Fotakis C 2011 Biomimetic micro/nanostructured functional surfaces for microfluidic and tissue engineering applications *Biomicrofluidics* **5** 013411

[40] Xue M S, Wang W F, Wang F J, Ou J F, Li C Q and Li W 2013 Understanding of the correlation between work function and surface morphology of metals and alloys *J. Alloys Compd.* **577** 1–5

[41] Watson G S, Watson J A, Hu S, Brown C L, Cribb B W and Myhra S 2010 Micro and nanostructures found on insect wings-designs for minimising adhesion and friction *Int. J. Nanomanuf.* **5** 112

[42] Zhang X, Shi F, Niu J, Y G J and Wang Z Q 2008 Superhydrophobic surfaces: from structural control to functional application *J. Mater. Chem.* **18** 621–33

[43] Nayak B K and Gupta M C 2010 Self-organized micro/nano structures in metal surfaces by ultrafast laser irradiation *Opt. Lasers Eng.* **48** 940–9

[44] Zhu S, Li J, Cai S, Bian Y, Chen C, Xu B, Su Y, Hu Y, Wu D and Chu J 2020 Unidirectional transport and effective collection of underwater CO_2 bubbles utilizing ultrafast-laser-ablated Janus foam *ACS Appl. Mater. Interfaces* **12** 18110–5

[45] Liu M J, Wang S T and Jiang L 2017 Nature-inspired superwettability systems *Nat. Rev. Mater.* **2** 17036

[46] Zhou H, Zhang M X, Li C, Gao C L and Zheng Y M 2018 Excellent fog-droplets collector via integrative janus membrane and conical spine with micro/nanostructures *Small* **14** 1801335

[47] Ionin A A, Kudryashov S I, Makarov S V, Seleznev L V, Sinitsyn D V, Golosov E V, Golosova O A, Kolobov Y R and Ligachev A E 2012 Femtosecond laser color marking of metal and semiconductor surfaces *Appl. Phys.* A **107** 301–5

[48] Suriano R, Kuznetsov A, Eaton S M, Kiyan R, Cerullo G, Osellame R, Chichkov B N, Levi M and Turri S 2011 Femtosecond laser ablation of polymeric substrates for the fabrication of microfluidic channels *Appl. Surf. Sci.* **257** 6243–50

[49] Cao L L, Jones A K, Sikka V K, Wu J Z and Gao D 2009 Anti-icing superhydrophobic coatings *Langmuir* **25** 12444–8

[50] Xue Z X, Cao Y Z, Liu N, Feng L and Jiang L 2014 Special wettable materials for oil/water separation *J. Mater. Chem.* A **2** 2445–60

[51] Hochbaum A I and Yang P D 2009 Semiconductor nanowires for energy conversion *Chem. Rev.* **110** 527–46

[52] Zhao Y J and Cho S K 2007 Micro air bubble manipulation by electrowetting on dielectric (EWOD): transporting, splitting, merging and eliminating of bubbles *Lab Chip* **7** 273–80

[53] Gu Z Z, Uetsuka H, Takahashi K, Nakajima R, Onishi H, Fujishima A and Sato O 2003 Structural color and the lotus effect *Angew. Chem. Int. Ed.* **42** 894–7

[54] Ghiradella H 1991 Light and color on the wing: structural colors in butterflies and moths *Appl. Opt.* **30** 3492–500

[55] Taniguchi T and Mibae J 1984 Anti-fogging coating film: *U.S. Patent*. 4478909

[56] Lai Y K, Tang Y X, Gong J J, Gong D G, Chi L F, Lin C and Chen Z 2012 Transparent superhydrophobic/superhydrophilic TiO_2-based coatings for self-cleaning and anti-fogging *J. Mater. Chem.* **22** 7420–6

[57] Popa-Lisseanu A G and Voigt C C 2009 Bats on the move *J. Mammal* **90** 1283–9

[58] Cheng Y T and Rodak D E 2005 Is the lotus leaf superhydrophobic? *Appl. Phys. Lett.* **86** 144101

[59] Hu D L, Chan B and Bush J W M 2003 The hydrodynamics of water strider locomotion *Nature* **424** 663–6

[60] Bhushan B and Nosonovsky M 2010 The rose petal effect and the modes of superhydrophobicity *Philos. Trans. R. Soc.* A **368** 4713–28

[61] Bohn H F and Federle W 2004 Insect aquaplaning: *nepenthes* pitcher plants capture prey with the peristome, a fully wettable water-lubricated anisotropic surface *Proc. Natl Acad. Sci. USA* **101** 14138–43

[62] Huang J Y, Wang X D and Wang Z L 2006 Controlled replication of butterfly wings for achieving tunable photonic properties *Nano Lett.* **6** 2325–31

[63] Stegmaier T, Linke M and Planck H 2009 Bionics in textiles: flexible and translucent thermal insulations for solar thermal applications *Phil. Trans. Roy. Soc.* A **367** 1749–58

[64] Hulteen J C and Van Duyne R P 1995 Nanosphere lithography: a materials general fabrication process for periodic particle array surfaces *J. Vac. Sci. Technol.* A **13** 1553–8

[65] Li X H, Abe T and Esashi M 2001 Deep reactive ion etching of Pyrex glass using SF6 plasma *Sensors Actuators* A **87** 139–45

[66] Grier D, Ben-Jacob E, Clarke R and Sander L M 1986 Morphology and microstructure in electrochemical deposition of zinc *Phys. Rev. Lett.* **56** 1264–7

[67] Tokuda M, Azuma J, Otsubo T, Yamaguchi Y and Sasaki I 1992 Processing apparatus and method for plasma processing *US Patent* 5134965

[68] Zhang Y L, Chen Q D, Xia H and Sun H B 2010 Designable 3D nanofabrication by femtosecond laser direct writing *Nano Today* **5** 435–48

[69] Kawata S, Sun H B, Tanaka T and Takada K 2001 Finer features for functional microdevices *Nature* **412** 697–8

[70] Lv X, Jiao Y L, Wu S Z, Li C Z, Zhang Y Y, Li J, Hu Y and Wu D 2019 Anisotropic sliding of underwater bubbles on microgrooved slippery surfaces by one-step femtosecond laser scanning *ACS Appl. Mater. Interfaces* **11** 20574–80

[71] Xin C *et al* 2019 Conical Hollow Microhelices with superior swimming capabilities for targeted cargo delivery *Adv. Mater.* **31** 1808226

[72] Hu Y L, Lao Z X, Cumming B P, Wu D, Li J W, Liang H, Chu J, Huang W and Gu M 2015 Laser printing hierarchical structures with the aid of controlled capillary-driven self-assembly *Proc. Natl Acad. Sci. USA* **112** 6876–81

[73] Serbin J, Egbert A, Ostendorf A, Chichkov B N, Houbertz R, Domann G, Schulz J, Cronauer C, Fröhlich L and Popall M 2003 Femtosecond laser-induced two-photon polymerization of inorganic–organic hybrid materials for applications in photonics *Opt. Lett.* **28** 301–3

[74] Lv J Y, Song Y L, Jiang L and Wang J J 2014 Bio-inspired strategies for anti-icing *ACS Nano* **8** 3152–69

[75] Zhang X Y, Li Z, Liu K S and Jiang L 2013 Bioinspired multifunctional foam with self-cleaning and oil/water separation *Adv. Funct. Mater.* **23** 2881–6

[76] Nozik A J 1978 Photoelectrochemistry: applications to solar energy conversion *Annu. Rev. Phys. Chem.* **29** 189–222

[77] Hu W Q, Ishii K S and Ohta A T 2011 Micro-assembly using optically controlled bubble microrobots *Appl. Phys. Lett.* **99** 094103

[78] Wu Z Z, Lee D, Rubner M F and Cohen R E 2007 Structural color in porous, superhydrophilic, and self-cleaning SiO_2/TiO_2 bragg stacks *Small* **3** 1445–51

[79] Zmoda B J and Brown R S 1974 Anti-fogging window cleaner surfactant mixture *US Patent* 3819522

[80] Razavi B and Behzad R 1998 *RF Microelectronics* (New Jersey: Prentice Hall)

[81] Herzig H P 2014 *Micro-Optics: Elements, Systems and Applications* (Boca Raton, FL: CRC Press)

[82] Teh S Y, Lin R, Hung L H and Lee A P 2008 Droplet microfluidics *Lab Chip* **8** 198–220

[83] Kósa G, Shoham M and Zaaroor M 2005 Propulsion of a swimming micro medical robot *Proc. 2005 IEEE Int. Conf. on Robotics and Automation* (Barcelona: IEEE) 1327–31

[84] Arai F, Ando D, Fukuda T, Nonoda Y and Oota T 1995 Micro manipulation based on micro physics-strategy based on attractive force reduction and stress measurement *Proc. 1995 IEEE/RSJ Int. Conf. on Intelligent Robots and Systems. Human Robot Interaction and Cooperative Robots* (Pittsburgh, PA: IEEE) pp 236–41

[85] Ehrfeld W, Hessel V and Löwe H 2000 *Microreactors: New Technology for Modern Chemistry.* (Weinheim: Wiley)

[86] Üneri A *et al* 2010 New steady-hand eye robot with micro-force sensing for vitreoretinal surgery *Proc. 2010 3rd IEEE RAS & EMBS Int. Conf. on Biomedical Robotics and Biomechatronics* (Tokyo: IEEE) pp 814–9

[87] Jacobsen S C, Wells D L, Davis C C and Wood J E 1991 Fabrication of micro-structures using non-planar lithography (NPL) *Proc. IEEE Micro Electro Mechanical Systems* (Piscataway, NJ: IEEE) pp 45–50

[88] Randolph S J, Fowlkes J D and Rack P D 2006 Focused, nanoscale electron-beam-induced deposition and etching *Crit. Rev. Solid State Mater. Sci.* **31** 55–89

[89] Young R J, Cleaver J R A and Ahmed H 1993 Characteristics of gas-assisted focused ion beam etching *J. Vac. Sci. Technol.* B **11** 234–41

[90] Cao Y, Andreatta A, Heeger A J and Smith P 1989 Influence of chemical polymerization conditions on the properties of polyaniline *Polymer* **30** 2305–11

[91] Grzelczak M, Vermant J, Furst E M and Liz-Marzán L M 2010 Directed self-assembly of nanoparticles *ACS Nano* **4** 3591–605

[92] Buividas R, Mikutis M, Kudrius T, Greičius A, Šlekys G and Juodkazis S 2012 Femtosecond laser processing - a new enabling technology *Lith. J. Phys.* **52** 301–11

[93] Jiang L, Wang A D, Li B, Cui T H and Lu Y F 2017 Electrons dynamics control by shaping femtosecond laser pulses in micro/ nanofabrication: modeling, method, measurement and application *Light Sci. Appl.* **7** 17134

[94] Chichkov B N, Momma C, Nolte S, Von Alvensleben F and Tünnermann A 1996 Femtosecond, picosecond and nanosecond laser ablation of solids *Appl. Phys.* A **63** 109–15

[95] Bonse J, Baudach S, Krüger J, Kautek W and Lenzner M 2002 Femtosecond laser ablation of silicon–modification thresholds and morphology *Appl. Phys.* A **74** 19–25

[96] Wang C W *et al* 2015 Consideration of femtosecond laser-induced effect on semiconductor material sic substrate for CMP processing *Appl. Mech. Mater.* **799–800** 458–62

[97] Qian F, *et al* 1996 Femtosecond laser deposition of diamond-like carbon films *Proc. Symp. Mater. Res. Soc.* **397** 297–302

[98] Kirichenko N A, Sukhov I A, Shafeev G A and Shcherbina M E 2012 Evolution of the distribution function of au nanoparticles in a liquid under the action of laser radiation *Quantum Electron.* **42** 175–80

[99] Paipulas D, Mizeikis V, Purlys V, Čerkauskaite A and Juodkazis S 2015 Volumetric integration of photorefractive micromodifications in lithium niobate with femtosecond laser pulses *Proc. SPIE* **9374** 93740B

[100] Odachi G, Sakamoto R, Hara K and Yagi T 2013 Effect of air on debris formation in femtosecond laser ablation of crystalline Si *Appl. Surf. Sci.* **282** 525–30

[101] Reif J, Varlamova O and Costache F 2008 Femtosecond laser induced nanostructure formation: self-organization control parameters *Appl. Phys.* A **92** 1019–24

[102] Andreev A V and Chalykh R A 2002 Nuclear excitation by x-ray emission of femtosecond laser plasma *Hyperfine Interact.* **143** 13–22

[103] Gauderon R, Lukins P B and Sheppard C J R 1998 Three-dimensional second-harmonic generation imaging with femtosecond laser pulses *Opt. Lett.* **23** 1209–11

[104] Li C, Cheng G H and Razvan S 2016 Investigation of femtosecond laser-induced periodic surface structure on tungsten *Acta Opt. Sin.* **36** 0532001

[105] Liang F, Lehr J, Danielczak L, Leask R and Kietzig A M 2014 Robust non-wetting PTFE surfaces by femtosecond laser machining *Int. J. Mol. Sci.* **15** 13681–96

[106] Shi X Y *et al* 2019 Quantitative assessment of structural and compositional colors induced by femtosecond laser: a case study on 301ln stainless steel surface *Appl. Surf. Sci.* **484** 655–62

[107] Besner S, Kabashin A V, Meunier M and Winnik F M 2005 Fabrication of functionalized gold nanoparticles by femtosecond laser ablation in aqueous solutions of biopolymers *Proc. SPIE* **5969** 59690B

[108] Bashir S, Rafique M S, Nathala C S and Husinsky W 2014 The formation of nanodimensional structures on the surface of tin exposed to femtosecond laser pulses in the ambient environment of ethanol *Appl. Surf. Sci.* **290** 53–58

[109] Ju Y F, Liu C N, Liao Y, Liu Y, Zhang L, Yinglong Shen Y S, Danping Chen D C and Ya Cheng Y C 2013 Direct fabrication of a microfluidic chip for electrophoresis analysis by water-assisted femtosecond laser writing in porous glass *Chin. Opt. Lett.* **11** 072201

[110] Golosov E V, Ionin A A, Kolobov Y R, Kudryashov S I, Ligachev A E, Makarov S V, Novoselov Y N, Seleznev L V, Sinitsyn D V and Sharipov A R 2011 Near-threshold femtosecond laser fabrication of one-dimensional subwavelength nanogratings on a graphite surface *Phys. Rev.* B **83** 115426

[111] De Ninno A, Gerardino A, Girarda B, Grenci G and Businaro L 2010 Top-down approach to nanotechnology for cell-on-chip applications *Biophys. Bioeng. Lett.* **32**

[112] Feng L G *et al* 2014 Electrocatalysts and catalyst layers for oxygen reduction reaction *Rotating Electrode Methods and Oxygen Reduction Electrocatalysts* ed W Xing, G P Yin and J J Zhang (Amsterdam: Elsevier) pp 67–132

[113] Hopwood J 1992 Review of inductively coupled plasmas for plasma processing *Plasma Sources Sci. Technol.* **1** 109–16

[114] Li G Q, Li J W, Zhang C C, Hu Y L, Li X H, Chu J, Huang W and Wu D 2015 Large-area one-step assembly of three-dimensional porous metal micro/nanocages by ethanol-assisted femtosecond laser irradiation for enhanced antireflection and hydrophobicity *ACS Appl. Mater. Interfaces* **7** 383–90

[115] Chen C, Shi L A, Huang Z C, Hu Y L, Wu S Z, Li J, Wu D and Chu J 2019 Microhole-arrayed PDMS with controllable wettability gradient by one-step femtosecond laser drilling for ultrafast underwater bubble unidirectional self-transport *Adv. Mater. Interfaces* **6** 1900297

[116] Ren F F *et al* 2017 A single-layer Janus membrane with dual gradient conical micropore arrays for self-driving fog collection *J. Mater. Chem.* A **5** 18403–8

[117] Li G Q *et al* 2016 Multifunctional ultrathin aluminum foil: oil/water separation and particle filtration *J. Mater. Chem.* A **4** 18832–40

[118] Zhang Z *et al* 2017 A Janus oil barrel with tapered microhole arrays for spontaneous high-flux spilled oil absorption and storage *Nanoscale* **9** 15796–803

[119] Yan S G *et al* 2018 Unidirectional self-transport of air bubble via a Janus membrane in aqueous environment *Appl. Phys. Lett.* **113** 261602

[120] Yong J L, Chen F, Fang Y, Huo J L, Yang Q, Zhang J, Bian H and Hou X 2017 Bioinspired design of underwater superaerophobic and superaerophilic surfaces by femtosecond laser ablation for anti-or capturing bubbles *ACS Appl. Mater. Interfaces* **9** 39863–71

[121] Chen C *et al* 2019 In situ reversible control between sliding and pinning for diverse liquids under ultra-low voltage *ACS Nano* **13** 5742–52

[122] Li M J, Yang Q, Chen F, Yong J L, Bian H, Wei Y, Fang Y and Hou X 2019 Integration of great water repellence and imaging performance on a superhydrophobic PDMS microlens array by femtosecond laser microfabrication *Adv. Eng. Mater.* **21** 1800994

[123] Bai X, Yang Q, Fang Y, Zhang J Z, Yong J L, Hou X and Chen F 2020 Superhydrophobicity-memory surfaces prepared by a femtosecond laser *Chem. Eng. J.* **383** 123143

[124] Lu Y, Yu L D, Zhang Z, Wu S Z, Li G Q, Wu P, Hu Y, Li J, Chu J and Wu D 2017 Biomimetic surfaces with anisotropic sliding wetting by energy-modulation femtosecond laser irradiation for enhanced water collection *RSC Adv.* **7** 11170–9

[125] Fang Y, Yong J L, Chen F, Huo J L, Yang Q, Zhang J and Hou X 2018 Bioinspired fabrication of bi/Tridirectionally anisotropic sliding Superhydrophobic PDMS

surfaces by femtosecond laser *Adv. Mater. Interfaces* **5** 1701245
[126] Zhang Y C *et al* 2018 Localized self-growth of reconfigurable architectures induced by a femtosecond laser on a shape-memory polymer *Adv. Mater.* **30** 1803072
[127] Li G Q, Li J W, Hu Y L, Zhang C C, Li X H, Chu J and Huang W 2015 Femtosecond laser color marking stainless steel surface with different wavelengths *Appl. Phys.* A **118** 1189–96
[128] Sakabe S, Hashida M, Tokita S, Namba S and Okamuro K 2009 Mechanism for self-formation of periodic grating structures on a metal surface by a femtosecond laser pulse *Phys. Rev.* B **79** 033409
[129] Li G Q, Zhang Z, Wu P C, Wu S Z, Hu Y L, Zhu W, Li J, Wu D, Li X and Chu J 2016 One-step facile fabrication of controllable microcone and micromolar silicon arrays with tunable wettability by liquid-assisted femtosecond laser irradiation *RSC Adv.* **6** 37463–71
[130] Li G Q, Lu Y, Wu P C, Zhang Z, Li J W, Zhu W, Hu Y, Wu D and Chu J 2015 Fish scale inspired design of underwater superoleophobic microcone arrays by sucrose solution assisted femtosecond laser irradiation for multifunctional liquid manipulation *J. Mater. Chem.* A **3** 18675–83
[131] Shen M Y, Carey J E, Crouch C H, Kandyla M, Stone H A and Mazur E 2008 High-density regular arrays of nanometer-scale rods formed on silicon surfaces via femtosecond laser irradiation in water *Nano Lett.* **8** 2087–91
[132] Petersen S, Barchanski A, Taylor U, Klein S, Rath D and Barcikowski S 2011 Penetratin-conjugated gold nanoparticles − design of cell-penetrating nanomarkers by femtosecond laser ablation *J. Phys. Chem.* C **115** 5152–9
[133] Barcikowski S and Compagnini G 2013 Advanced nanoparticle generation and excitation by lasers in liquids *Phys. Chem. Chem. Phys.* **15** 3022–6
[134] Kabashin A V, Meunier M, Kingston C and Luong J H T 2003 Fabrication and characterization of gold nanoparticles by femtosecond laser ablation in an aqueous solution of cyclodextrins *J. Phys. Chem.* B **107** 4527–31
[135] Sylvestre J P *et al* 2004 Surface chemistry of gold nanoparticles produced by laser ablation in aqueous media *J. Phys. Chem.* B **108** 16864–9
[136] Amendola V, Polizzi S and Meneghetti M 2006 Laser ablation synthesis of gold nanoparticles in organic solvents *J. Phys. Chem.* B **110** 7232–7
[137] Amendola V, Polizzi S and Meneghetti M 2007 Free silver nanoparticles synthesized by laser ablation in organic solvents and their easy functionalization *Langmuir* **23** 6766–70
[138] Albu C, Dinescu A, Filipescu M, Ulmeanu M and Zamfirescu M 2013 Periodical structures induced by femtosecond laser on metals in air and liquid environments *Appl. Surf. Sci.* **278** 347–51
[139] Shen M Y, Crouch C H, Carey J E and Mazur E 2004 Femtosecond laser-induced formation of submicrometer spikes on silicon in water *Appl. Phys. Lett.* **85** 5694–6
[140] Gundlach E R and Hayes M O 1978 Vulnerability of coastal environments to oil spill impacts *Mar. Technol. Soc. J.* **12** 18–27
[141] Uriell C W 1953 Air float jogger device *US Patent* 2626801
[142] Falconer A 2003 Gravity separation: old technique/new methods *Phys. Sep. Sci. Eng.* **12** 812865
[143] Sammons J K and Fox C H Jr 1979 Centrifugal water oil separator *US Patent* 4175040
[144] Yin K, Chu D K, Dong X R, Wang C, Duan J A and He J 2017 Femtosecond laser induced robust periodic nanoripple structured mesh for highly efficient oil–water separation *Nanoscale* **9** 14229–35
[145] Kostal E, Stroj S, Kasemann S, Matylitsky V and Domke M 2018 Fabrication of biomimetic fog-collecting superhydrophilic–superhydrophobic surface micropatterns using femtosecond lasers *Langmuir* **34** 2933–41
[146] Yin K, Yang S, Dong X R, Chu D K, Duan J A and He J 2018 Ultrafast achievement of a superhydrophilic/hydrophobic Janus foam by femtosecond laser ablation for directional water transport and efficient fog harvesting *ACS Appl. Mater. Interfaces* **10** 31433–40
[147] Yin K, Du H F, Dong X R, Wang C, Duan J A and He J 2017 A simple way to achieve bioinspired hybrid wettability surface with micro/nanopatterns for efficient fog collection *Nanoscale* **9** 14620–6
[148] Volat C, Farzaneh M and Leblond A 2005 De-icing/anti-icing techniques for power lines: current methods and future direction. *Proc. 11th International Workshop on Atmospheric Icing of Structures* (Montreal)
[149] Parent O and Ilinca A 2011 Anti-icing and de-icing techniques for wind turbines: critical review *Cold Reg. Sci. Technol.* **65** 88–96
[150] Chang H, Shi Y, W Y Y and Zhang M 2008 Ice-melting technologies for HVAC and HVDC transmission line *Power Syst. Technol.* **5** 1–6
[151] Long J Y, Wu Y C, Gong D W, Fan P X, Jiang D F, Zhang Hongjun Z and Zhong M 2015 Femtosecond laser fabricated superhydrophobic copper surfaces and their anti-icing properties *Chin. J. Lasers* **42** 0706002
[152] Li G Q, Li J W, Hu Y L, Zhang C C, Li X H, Chu J and Huang W 2014 Realization of diverse displays for multiple color patterns on metal surfaces *Appl. Surf. Sci.* **316** 451–5
[153] Geng H Y and Cho S K 2018 Dielectrowetting for digital microfluidics *Advances in Contact Angle, Wettability and Adhesion* ed K L Mittal (Austin, TX: Scrivener) **3** pp 193–218
[154] Seo K S, Wi R, Im S G and Kim D H 2013 A superhydrophobic magnetic elastomer actuator for droplet motion control *Polym. Adv. Technol.* **24** 1075–80
[155] Xu X P and Qian T Z 2012 Thermal singularity and droplet motion in one-component fluids on solid substrates with thermal gradients *Phys. Rev.* E **85** 061603
[156] Chen C, Huang Z C, Shi L A, Jiao Y L, Zhu S W, Li J, Hu Y, Chu J, Wu D and Jiang L 2019 Remote photothermal actuation of underwater bubble toward arbitrary direction on planar slippery Fe_3O_4-doped surfaces *Adv. Funct. Mater.* **29** 1904766
[157] Zhang Y, Jiao Y L, Chen C, Zhu S W, Li C Z, Li J, Hu Y, Wu D and Chu J 2019 Reversible tuning between isotropic and anisotropic sliding by one-direction mechanical stretching on microgrooved slippery surfaces *Langmuir* **35** 10625–30
[158] Jiao Y L *et al* 2019 Pitcher plant-bioinspired bubble slippery surface fabricated by femtosecond laser for buoyancy-driven bubble self-transport and efficient gas capture *Nanoscale* **11** 1370–8
[159] Yong J L, Huo J L, Yang Q, Chen F, Fang Y, Wu X, Liu L, Lu X, Zhang J and Hou X 2018 Femtosecond laser direct writing of porous network microstructures for fabricating super-slippery surfaces with excellent liquid repellence and anti-cell proliferation *Adv. Mater. Interfaces* **5** 1701479

[160] Fan P X, Bai B F, Zhong M L, Zhang H J, Long J Y, Han J, Wang W and Jin G 2017 General strategy toward dual-scale-controlled metallic micro–nano hybrid structures with ultralow reflectance *ACS Nano* **11** 7401–8
[161] Vorobyev A Y and Guo C L 2011 Antireflection effect of femtosecond laser-induced periodic surface structures on silicon *Opt. Express* **19** A1031–6
[162] Vorobyev A Y and Guo C L 2011 Direct creation of black silicon using femtosecond laser pulses *Appl. Surf. Sci.* **257** 7291–4
[163] Zhang S, Hu X N, Liao Y, He F, Liu C N and Ya Cheng Y C 2013 Microstructuring of anti-reflection film for HgCdTe/Si IRFPA with femtosecond laser pulse *Chin. Opt. Lett.* **11** 033101